Describing Function Error Bounds

-The Non-Autonomous Case

A Thesis

Presented to

the Faculty of Graduate Studies and Research

The University of Manitoba

In Partial Fulfillment

of the Requirements for the Degree

Master of Science

by

Barrie William Leach

October 1968

ABSTRACT

by

Barrie William Leach

Describing Function Error Bounds
-the Non-Autonomous Case

The application of various describing function error estimate techniques to first and second order systems was investigated. Emphasis was placed on the application of these estimate techniques to practical systems in their normal operating region. Experimental results by analog simulation were used in a comparison of the various bounds as applied to first order systems. Applicability of the estimate techniques to second order systems was correlated with the amount of resonance in the linear transfer function of the system, and a few experimental findings were used in a comparison of estimates for the second order case. Results revealed that all estimate techniques considered were far from being of practical use to the designer of nonlinear control systems.

ACKNOWLEDGEMENTS

I wish to thank my thesis advisor, Professor R. A. Johnson of the Department of Electrical Engineering, the University of Manitoba, for his many helpful suggestions and general encouragement during this investigation. Thanks must also be extended to the National Research Council of Canada for its financial assistance, and to my wife, Marjorie, for her patient understanding and her help in typing this thesis.

TABLE OF CONTENTS

CHAPTER PAGE

CHAPTER PAGE

LIST OF TABLES AND FIGURES

CHAPTER I

INTRODUCTION AND FORMULATION OF THE PROBLEM

I. THE DESCRIBING FUNCTION METHOD

Definition of the describing function[1]

Consider the single-loop nonlinear feedback system of Figure 1. G(s) represents the transfer function of the linear portion of the loop and N represents a single nonlinear element with a transfer characteristic

$$m = f(e). \qquad \text{(I-1)}$$

It is convenient to consider the nonlinear function, f(e), as consisting of two parts (a quasilinear gain and a distortion term) of the form

$$f(e) = K_{eq}e + f_d(e). \qquad \text{(I-2)}$$

With e assumed to be a sinusoidal input, $K_{eq}e$ represents the fundamental component of the output of the nonlinearity while $f_d(e)$ is the distortion component. K_{eq} will be a function of the input signal amplitude, and becomes the describing function for f(e). The conventional sinusoidal describing function is chosen so as to minimize $f_d(e)$ in the mean-square sense, and hence becomes the Fourier series coefficient of the fundamental of the output of the

---

[1] John E. Gibson, Nonlinear Automatic Control (New York: McGraw-Hill Book Company, Inc., 1963), pp. 344-347.

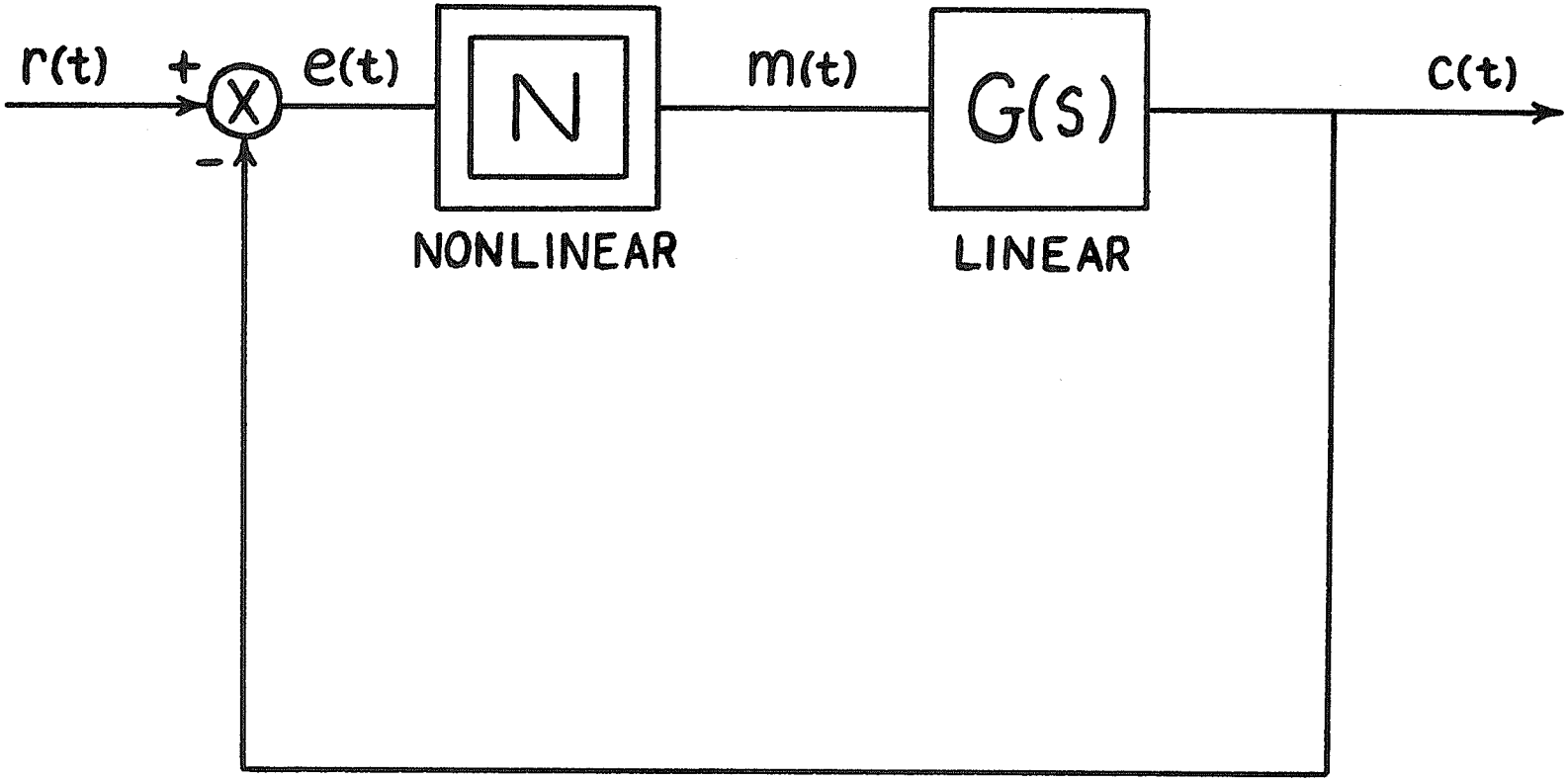

FIGURE 1

NONLINEAR FEEDBACK SYSTEM

nonlinearity divided by the amplitude of the input fundamental, E. Thus, for a sinusoidal input:

$$e = E \sin(wt) = E \sin(\theta_1) , \qquad \text{(I-3)}$$

the normalized fundamental terms,

$$g(E) = \frac{1}{\pi E} \times \int_0^{2\pi} f[E \sin(\theta_1)] \sin(\theta_1) d\theta_1 \qquad \text{(I-4a)}$$

and

$$b(E) = \frac{1}{\pi E} \times \int_0^{2\pi} f[E \sin(\theta_1)] \cos(\theta_1) d\theta_1 , \qquad \text{(I-4b)}$$

are defined. Then the describing function, K_{eq}, becomes,

$$K_{eq} = g(E) + jb(E) . \qquad \text{(I-5)}$$

For symmetric single-valued nonlinearities b(e) will be zero. This definition of the conventional sinusoidal describing function will be implied throughout.

Use of the describing function in forced systems

The describing function can be used under certain conditions to predict the approximate closed-loop frequency response and relative stability of nonautonomous nonlinear systems of the form in Figure 1. For example, if r(t) (referring to Figure 1) is a sinusoidal input, R sin wt, and the linear harmonic transfer function, G(jw), is sufficiently low pass, then the error signal, e, can be approximated as a fundamental sinusoid, $\hat{e}(t)$, where

$$\hat{e}(t) = E \sin(wt + \theta). \qquad \text{(I-6)}$$

A closed-loop transfer function relating e(t) to r(t) then can be written as

$$\frac{\hat{e}(jw)}{r(jw)} = \frac{1}{1 + K_{eq} G(jw)} . \qquad \text{(I-7)}$$

This yields a magnitude relationship,

$$\frac{E}{R} = \left| \frac{1}{1 + K_{eq}(E)G(jw)} \right| , \qquad \text{(I-8)}$$

and a phase relationship

$$\theta = \angle \frac{1}{1 + K_{eq}(E)G(jw)} . \qquad \text{(I-9)}$$

If the nonlinearity is symmetric and single-valued then

$$K_{eq} = g(E) , \qquad \text{(I-10)}$$

and $K_{eq}(E)$ is a real function of E. Equation (I-8) can then be solved readily for $K_{eq}(E)$. The right hand side of the resulting equation will be a function of R, E, G, and w. For given G(jw) and R, the right hand side can be plotted versus E for various w. The left hand side plotted versus E is simply the describing function of the nonlinearity. Possible operating points (E,w) of the system are found as the intersections of the two curves.[2] With E known, $|c(t)|$ can be plotted versus w for given R, yielding the closed loop response.

Alternatively, equation (I-8) could be inverted and rewritten as

$$R = E \left| 1 + K_{eq}(E)G(jw) \right| . \qquad \text{(I-11)}$$

For specified E, R and θ (equation I-9) can be found quite readily at any given frequency. In this way, the operating points can be found in a straightforward computational manner, rather than by resorting to graphical techniques.

---

[2] For example plots see Gibson, op. cit., pp. 393-394.

Garber[3] outlines the first approximation in Galerkin's method as the equivalent to the foregoing describing function method. The results are the same except that any ambiguity in calculating the angle θ is erased with the use of the first approximation in Galerkin's method.

Further details of the application of the describing function method to forced systems can be found in texts by Truxal[4] and Gibson[5].

Inherent assumptions and inaccuracies of the method

Two basic assumptions in the application of the describing function method are readily apparent from the development of the definition of the describing function using the system of Figure 1. First of all, the system may contain only one nonlinear element. Secondly, the nonlinear element may not change its characteristic with time. The third assumption is that, if the input to the nonlinearity is a sinusoid, then only the fundamental component of the nonlinearity is significant in the feedback loop. This assumption is known as the filter hypothesis, and forms

---

[3] E. D. Garber, "Error Estimation in the Describing Function Method", Automation and Remote Control, Vol. 24, 1963, pp. 449-450.

[4] John G. Truxal, Automatic Feedback Control System Synthesis (New York: McGraw-Hill Book Company, Inc., 1955), pp. 581-585.

[5] Gibson, op. cit., pp. 389-395.

the basis for the use of the describing function. Intuitively, if no subharmonic components are present in the system, then the filter hypothesis can be justified by the fact that higher harmonics in the output of the nonlinearity usually have smaller amplitudes than the fundamental,and most linear elements exhibit low-pass filter characteristics which tend to attenuate the higher harmonics.

Obviously, no practical linear element will act as a perfect low-pass filter. Some harmonic content will always be fed back to the input of the nonlinearity, thus rendering the describing function method an approximation only.

The degree of approximation can only be surmised in a lot of cases, so practical use of the describing function must remain suspect until some investigation into the error involved in its use has taken place.

For a complete discussion of the definition, use, and inaccuracies of the describing function, the reader is referred to bibliography references (4),(5),(6), and (15).

II. The Problem

Statement of the problem

Since about 1960,a number of articles have come forth yielding various techniques for determining bounds on the error involved in using the describing function.

This investigation was originally intended as a study of those techniques applying to non-autonomous (forced) systems. The techniques were to be applied to various systems of a general nature, with the hope that a comparison of techniques for various systems would yield such information as which bound technique should be applied to a given system. The determination of which bound to use would be made by considering both the ease of application and accuracy of the bounds.

Importance of the study

The describing function plays an important role in the analysis of nonlinear feedback systems because of its analogy with the frequency response methods of linear systems, and its relative ease of application. However, to be of practical use in the design of nonlinear feedback systems, it is necessary that some means of determining the error in application of the describing function method be available to the designer. Johnson[6] even questions the validity of applying the describing function method at all to non-autonomous systems without investigation into the errors involved. Ideally, the designer would like to be able to apply simple, but accurate, bound techniques to his problem, in order to determine whether or not the describing function

---

[6] E. C. Johnson, "Sinusoidal Analysis of Feedback-Control Systems Containing Nonlinear Elements", Trans. AIEE, Vol. 71, Part II. Applications and Industry, July, 1952, pp. 169-181.

method will be accurate enough for his work. Assuming this were possible, he could then study higher order systems by the approximate technique of reducing them to their dominant poles. The reduced system would supposedly be much easier for application of the describing function error estimates, and the estimates would give the designer some idea of the error involved in applying the describing function method to the original system. It must be stressed, however, that this type of design technique would rely heavily on the existence of fairly accurate error bound methods.

Because of the need for practical design techniques like the foregoing, the investigation of existing describing function error estimate techniques becomes important. The importance is further enhanced by the fact that the articles describing the various error bound techniques do not indicate the accuracy of their bounds.

CHAPTER II

REVIEW OF THE LITERATURE

Literature pertaining to non-autonomous systems

Sandberg[1] makes use of functional analysis to study a wide class of nonlinear control systems with one memoryless nonlinear element. An upper bound on the mean-square error resulting from the use of the describing function is found. As well, conditions are presented for the nonexistence of subharmonics and self-sustained oscillations.

Holtzman[2] indicates a technique for verifying whether or not an exact periodic solution of a forced nonlinear system exists in the neighbourhood of a periodic solution predicted by the describing function method. Again, functional analysis is used, but no applicable error bound is found.

Rozenvasser[3] has studied the exact determination of forced periodic oscillations in systems with a single piecewise linear nonlinearity. No error bounds are obtained

---

[1] I. W. Sandberg, "On the Response of Nonlinear Control Systems to Periodic Input Signals," The Bell System Technical Journal, Vol. XLIII, No. 3, May 1964, pp. 911-926.

[2] J. M. Holtzman, "Contraction Maps and Equivalent Linearization", The Bell System Technical Journal, Vol. XLVI, No. 10, December 1967, pp. 2405-2435.

[3] E. N. Rozenvasser, "On the Accurate Determination of Periodic Regimes in Sectionally Linear Automatic Control Systems", Automation and Remote Control, Vol. 21, 1960, pp. 902-910.

for the describing function method, but the work is important as a basis for subsequent papers.

Garber[4] studies the problem of determining the periodic state of forced oscillations in nonlinear systems. Describing function error estimates are found for certain constraints on the nonlinearity. The development is extended to the case of an automatic optimizing system described by equations with periodic coefficients.

A joint Garber and Rozenvasser[5] article develops estimates for the forced system case essentially the same as those given by Garber. The only improvements are in notation and extension of the technique to other systems.

Direction of the investigation

The three articles yielding forced system describing function error estimates of a usable type were those by Sandberg, Garber, and Garber and Rozenvasser. Since the Garber estimate and the Garber-Rozenvasser estimates were esentially the same, a comparison of Sandberg's estimate with that of the Garber-Rozenvasser article would be sufficient. This would then be a straightforward comparison of two methods and, hopefully, would determine which of the two estimates to use for a given system.

---

[4]Garber, op. cit.

[5]E. D. Garber and E. N. Rozenvasser, "The Investigation of Periodic Regimes of Nonlinear Systems on the Basis of the Filter Hypothesis", Automation and Remote Control, Vol. 26, 1965, pp. 274-285.

It was thought that the investigation should be started for systems with first order[6] linear transfer functions and then expanded to the second order case. Certainly, investigation of the second order case would be of more practical value, but the first order case was thought to offer a simple introduction to the estimate techniques. One nonlinearity was chosen at the outset as being fairly representative of a continuous[7] nonlinearity of practical use in control systems. This was the unit saturation nonlinearity expressed mathematically by,

$$f(e) = e \quad , \quad |e| \leq 1$$
$$f(e) = -1 \quad , \quad e \leq -1$$
$$f(e) = 1 \quad , \quad e \geq 1 \; . \qquad \text{(II-1)}$$

The Sandberg estimate

Sandberg uses functional analysis and, particularly, the contraction-mapping fixed-point theorem to develop his estimates. A few mathematical preliminaries are given in the article, but a more extensive coverage of functional analysis in general can be found in bibliography references (9), (10), (11), and (16).

---

[6] The order of a linear transfer function is the number of poles.

[7] All the error estimates considered required the nonlinear element to be continuous.

The space of real-valued periodic functions of t with period T which are square-integrable over a period (the space is denoted by K) is considered. The norm of any function g existing in K (norm denoted by $\| g \|$) is defined by

$$\| g \|^2 = \frac{1}{T} \int_0^T g^2 dt. \qquad \text{(II-2)}$$

This is recognized as simply the rms value of g.

The nonlinear control system considered is as shown in Figure 2. F is a linear operator operating on the output, v(t), of the nonlinearity Ψ. The input and output of the system are y and x respectively. I denotes the identity operator and w(t) is the input to the nonlinearity. Thus y is related to x by the functional equation

$$x = F\Psi[x + y] \ . \qquad \text{(II-3)}$$

$\mathcal{F} = \{ \ldots, F_{-1}, F_0, F_1, \ldots \}$ is a countable set of complex constants such that $\sup_n | F_n | < \infty$, and F_n is equal to the complex conjugate of F_{-n}. It is assumed that the restriction of F to K is a bounded linear mapping of K into itself, with the property that if $g \in K$ and $h = Fg$, then $h_n = F_n g_n$, where g_n and h_n are the n^{th} Fourier coefficients of g and h respectively.

An important special case,

$$Fg = \int_{-\infty}^{+\infty} f(t - \tau) g(\tau) d\tau \ , \quad g \in K \qquad \text{(II-4)}$$

where $f(t) \in L_{1R}$[8], is noted. This is the familiar convolution

---

[8] L_{1R} denotes the space of real-valued absolutely integrable functions defined on $(-\infty, \infty)$.

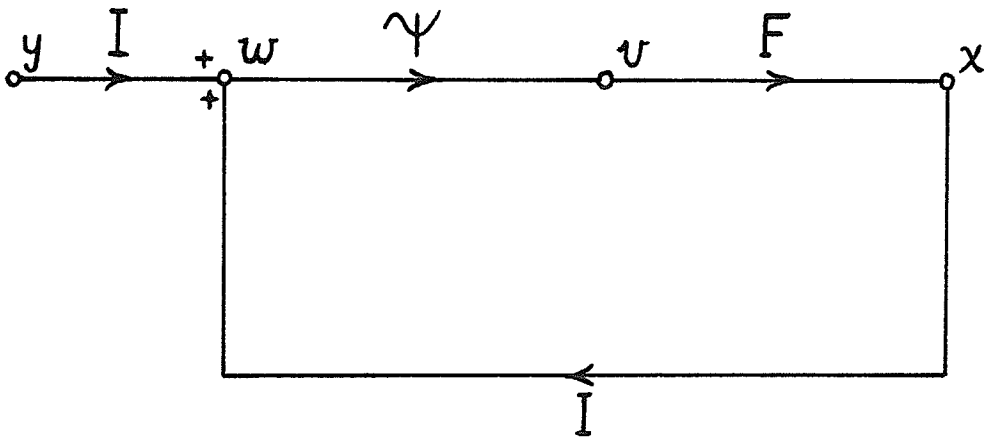

FIGURE 2

SANDBERG FEEDBACK SYSTEM

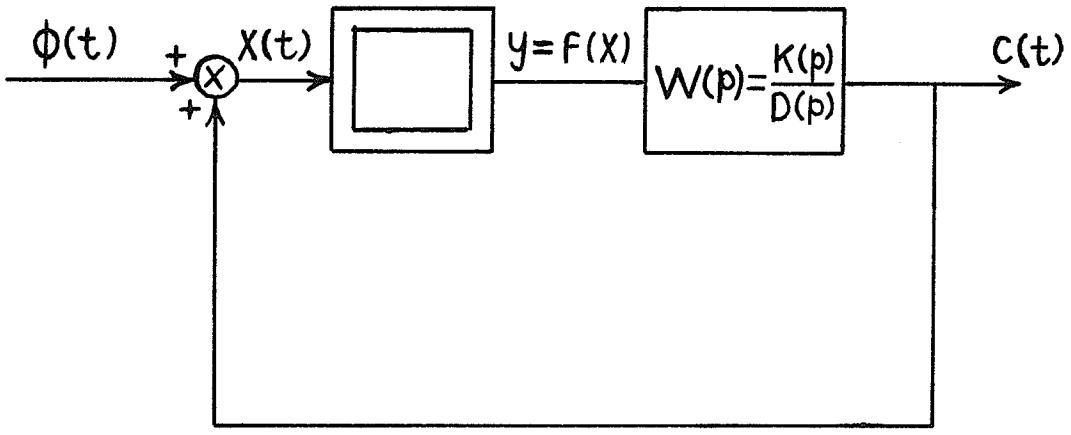

FIGURE 3

GARBER-ROZENVASSER FEEDBACK SYSTEM

integral of f and g, and hence F_n is found as $F(jnw_o)$, where $F(jw)$[9] is the Fourier transform of f(t).

The nonlinear function Ψ is assumed to be real-valued, independent of t, and such that there exist real constants α and β $(\beta > 0)$ with the properties that

$$\frac{1}{2}(\alpha + \beta) = 1 \qquad \text{(II-5)}$$

and

$$\alpha(\mu_1 - \mu_2) \leq \Psi(\mu_1) - \Psi(\mu_2) \leq \beta(\mu_1 - \mu_2) \qquad \text{(II-6)}$$

for any real $\mu_1 \geq \mu_2$.

It is observed that the application of the describing function technique to the system of Figure 2 amounts to analyzing the approximate system resulting from replacing F by the operator $\tilde{F}$, defined by,

$$\frac{1}{T}\int_0^T [\tilde{F}g]e^{-jnw_o t}\,dt = F_n g_n, \quad n = \pm 1$$
$$= 0, \quad n \neq \pm 1. \qquad \text{(II-7)}$$

Here $g \in K$; g_n is the n^{th} Fourier coefficient of g; and $T = \frac{2\pi}{w_o}$ is the period of the input sinusoid.

The projection operator, P, is a linear mapping of K into itself defined by

$$\frac{1}{T}\int_0^T [Pg]e^{-jnw_o t}\,dt = g_n, \quad n \in \mathcal{N}$$
$$= 0, \quad n \notin \mathcal{N}; \qquad \text{(II-8)}$$

where $\mathcal{N}$ is a set of integers such that $-m \in \mathcal{N}$ if $m \in \mathcal{N}$, and

---

[9] $F(jw)$ is defined here as $\int_{-\infty}^{+\infty} f(t)e^{-jwt}\,dt$.

$g \epsilon K$. In the case of main interest, $\mathcal{N} = \{-1, 1\}$, and $PF = \tilde{F}$.

Sandberg proves a number of theorems and corollaries. Those directly related to the error bound are stated below, and the reader is referred to the Sandberg paper for their proof.[10] A preliminary result is given as

Theorem I:

$$\| F \| = \sup_n | F_n | . \qquad \text{(II-9)}$$

If $\inf_n | 1 - F_n | > 0$, the operator (I-F) possesses a bounded inverse on K and

$$\| (I-F)^{-1} F \| = \sup_n | F_n/(1-F_n) | . \qquad \text{(II-10)}$$

The major result is

Theorem II: F, Ψ, and β are defined as before. Let $y \in K$. Suppose that

$$r = \sup_n | F_n/(1-F_n) | (\beta - 1) < 1 . \qquad \text{(II-11)}$$

Then there exists a unique $x \in K$ such that $x = F \Psi[x + y]$. In fact, $x = \lim_{m \to \infty} x_m$ where

$$x_{m+1} = (I-F)^{-1} F \{ \Psi[x_m + y] - x_m \}, \qquad \text{(II-12a)}$$

and x_0 is an arbitrary element of K. The m^{th} approximation, x_m, satisfies

$$\| x_m - x \| \leq \frac{r^m}{1-r} \| x_1 - x_0 \| . \qquad \text{(II-12b)}$$

A consequence of Theorem II is

Corollary II: Suppose that the hypotheses of TheoremII are satisfied and that $\hat{x} \in K$ satisfies $\hat{x} = PF \Psi[\hat{x} + y]$. Then

---

[10] The numbering of theorems and corollaries follows that of the Sandberg article.

$$\|x-\hat{x}\| \leq \frac{1}{1-r} \|(I-F)^{-1}F(I-P)\,\Psi[\hat{x}+y]\|. \qquad \text{(II-13)}$$

Sandberg notes that the hypotheses of Theorem II imply that there exists a unique $\hat{x}\in K$ such that $\hat{x} = PF\Psi[\hat{x}+y]$. Parseval's identity is used to develop the bound on $\|x-\hat{x}\|$ as,

$$\|x-\hat{x}\| \leq \frac{1}{1-r}\left\{\sum_{n\notin\pi}\left|\frac{F_n}{1-F_n}P_n\right|^2\right\}^{\frac{1}{2}}, \qquad \text{(II-14)}$$

where P_n is the n^{th} Fourier coefficient of $\Psi[\hat{x}+y]$. In the normal describing function case, $\pi = \{-1, 1\}$, and $y(t)$ is a sinusoid of period T. Also, if Ψ is an odd function, then $p_o = 0$. According to Sandberg, it can be shown that if $\alpha \geq 0, \Psi(0) = 0$, and $y = Py$ then,

$$\|P\Psi[\hat{x}+y]\| \geq \alpha\|\hat{x}+y\|; \qquad \text{(II-15)}$$

so that,

$$\begin{aligned}(I-P)\Psi[\hat{x}+y] &= \left(\|\Psi[\hat{x}+y]\|^2 - \|P\Psi[\hat{x}+y]\|^2\right)^{\frac{1}{2}} \\ &\leq (\beta^2-\alpha^2)^{\frac{1}{2}}\|\hat{x}+y\|.\end{aligned} \qquad \text{(II-16)}$$

Then the bound on $\|x-\hat{x}\|$ becomes

$$\begin{aligned}\|x-\hat{x}\| &\leq \frac{1}{1-r}\|(I-F)^{-1}F\| \cdot \|(I-P)\,\Psi[\hat{x}+y]\| \\ &\leq \frac{1}{1-r}\sup_{n\notin\pi}\left|\frac{F_n}{1-F_n}\right|(\beta^2-\alpha^2)^{\frac{1}{2}}\|\hat{x}+y\|.\end{aligned} \qquad \text{(II-17)}$$

As a special case, F' is defined as the restriction of F to the subspace

$$K' = \left\{g \mid g\in K;\ \int_0^T g(t)e^{-jnw_o t}\,dt = 0,\ n \text{ even}\right\} \qquad \text{(II-18)}$$

This gives rise to

Theorem IV: Let F' and K' be as defined above. Let Ψ and β be as defined before with the further qualification

that $\Psi(-\mu) = -\Psi(\mu)$ for any real μ (i.e. Ψ is odd symmetric). Suppose that

$$q = \sup_{n \text{ odd}} \left| \frac{F_n}{1-F_n} \right| (\beta - 1) < 1. \qquad \text{(II-19)}$$

Then the conclusion of Theorem II remains valid if K is replaced with K', r is replaced with q, and F is replaced with F'.

The Garber-Rozenvasser estimate

Garber and Rozenvasser consider the system

$$x = W(p)y + \phi = \frac{K(p)}{D(p)} y + \phi; (y = f(x)) \qquad \text{(II-20)}$$

as shown in Figure 3. W(p) is the transfer function of the linear part of the system, and is assumed to be a ratio of the two polynomials, K(p) and D(p), with K(P) of lower degree than D(p) (for physical realizability). The forcing function, $\phi(t)$, is a periodic function of the frequency w. The non-linearity is f(x), and is assumed piecewise continuous and such that

$$x(t+T) = x(t); \quad x(t+T/2) = -x(t), \qquad \text{(II-21)}$$

where $T = 2\pi/w$. If f(x) is assumed odd symmetric it can be shown[11] that x(t) is the solution of the integral equation

$$x(t) = \int_0^{T/2} \Phi(t-\tau) f\left[x(\tau)\right] d\tau + \phi(t), \qquad \text{(II-22)}$$

where the kernel, $\Phi(t-\tau)$, is given by

$$\Phi(t-\tau) = \frac{w}{\pi} \sum_{s=-\infty}^{\infty} W\left[(2s+1)jw\right] e^{(2s+1)jw(t-\tau)}. \qquad \text{(II-23)}$$

---

[11] Rozenvasser, op. cit.

Now the infinite series (II-23) can be expressed as a finite series by a complex variable technique described in Moretti.[12] The result is

$$\Phi(t-\tau)=\sum_{\rho=1}^{n} \frac{K(\lambda_\rho)}{D'(\lambda_\rho)} \frac{\exp[\lambda_\rho(t-\tau)]}{1+\exp\left[\frac{\pi\lambda_\rho}{w}\right]}; \quad (0 \leq t-\tau \leq \frac{\pi}{w}) \tag{II-24a}$$

$$= -\sum_{\rho=1}^{n} \frac{K(\lambda_\rho)}{D'(\lambda_\rho)} \frac{\exp[\lambda_\rho(\pi/w+t-\tau)]}{1+\exp[\pi\lambda_\rho/w]}; \quad (0 \leq \tau-t \leq \frac{\pi}{w}) \tag{II-24b}$$

where λ_ρ ($\rho = 1, 2, \ldots, n$) are the roots of the equation $D(\lambda) = 0$, and the roots are assumed to be simple.

Application of the describing function method to the system of Figure 3 will result in an approximate periodic regime, $x_{app}(t)$, for $x(t)$; and $x_{app}(t)$ will satisfy

$$x_{app}(t) = \int_0^{T/2} \Phi_1(t-\tau) f\left[x_{app}(\tau)\right] d\tau + \phi_1(t), \tag{II-25}$$

where

$$\Phi_1 = \frac{w}{\pi}\left\{W(jw)e^{jw(t-\tau)} + W(-jw)e^{-jw(t-\tau)}\right\} \tag{II-26}$$

is the fundamental component of the kernel Φ, and ϕ_1 is the fundamental component of the forcing function $\phi(t)$.

Subtraction of equation (II-26) from equation (II-22) together with some transformations yields

$$|x(t) - x_{app}(t)| \leq |J_1(t)| + |J_2(t)| \tag{II-27}$$

where

$$J_1(t) = \phi - \phi_1 + \int_0^{T/2} \Phi_h(t-\tau) f\left[x_{app}(\tau)\right] d\tau \tag{II-28}$$

and

$$J_2(t) = \int_0^{T/2} \Phi(t-\tau)\left\{f[x(\tau)] - f\left[x_{app}(\tau)\right]\right\} d\tau, \tag{II-29}$$

---

[12] Gino Moretti, Functions of a Complex Variable (Englewood Cliffs: Prentice-Hall, Inc., 1964), pp. 159-160.

with $\Phi_h = \Phi - \Phi_1$ as the sum of the higher harmonics of the kernel Φ.

If f(x) satisfies the uniform Lipschitz condition

$$\left|f(\xi_1)-f(\xi_2)\right| \leq M\left|\xi_1-\xi_2\right| ; \ (M = \text{const}) \qquad \text{(II-30)}$$

then a final estimate can be found in the form

$$\left|x - x_{app}\right| \leq \frac{\max|J_1|}{1 - MI} , \qquad \text{(II-31)}$$

where

$$I(w) = \int_0^{T/2} |\Phi(u)| \, du . \qquad \text{(II-32)}$$ [13]

The condition for applicability of estimate (II-31) is

$$1 - MI > 0 . \qquad \text{(II-33)}$$

Although Garber and Rozenvasser do not give specific details on the evaluation of $\max|J_1(t)|$, they say that an upper bound on $J_1(t)$ can be obtained rather simply. They do a simple example in which the exact value of $\max|J_1(t)|$ can be calculated quite readily. On the other hand, in Garber's paper is indicated an approximation to $\max|J_1(t)|$ made in one of his examples. The generalization of this approximation is as follows:

$$|J_1(t)| \overset{14}{=} \left|\int_0^{T/2} \left\{\Phi(t-\tau)-\Phi_1(t-\tau)\right\} f\left[x_{app}(\tau)\right] d\tau\right|$$

$$\leq \left\{\max_{0 \leq \tau \leq T/2} \left|f\left[x_{app}(\tau)\right]\right|\right\} \int_0^{T/2} \left|\Phi(t-\tau)-\Phi_1(t-\tau)\right| \left|d\tau\right|$$

---

[13] This is based on the fact that $\Phi(t-\tau+T/2) = -\Phi(t-\tau)$.

[14] This is assuming that $\phi(t) = \phi_1(t)$ (i.e. the input is sinusoidal). Then $J_1(t)$ is simply the response of the linear part of the system to the higher harmonics of the approximate output of the nonlinearity, $f\left[x_{app}(t)\right]$.

$$\leq \left\{ \max_{0 \leq \tau \leq T/2} \left| f\left[x_{app}(\tau) \right] \right| \right\} \int_0^{T/2} \left| \Phi(u) - \Phi_1(u) \right| du, \tag{II-34}$$

so that

$$\max_{0 \leq t \leq T/2} \left| J_1(t) \right| \leq \left\{ \max_{0 \leq \tau \leq T/2} \left| f\left[x_{app}(\tau) \right] \right| \right\} \int_0^{T/2} \left| \Phi(u) - \Phi_1(u) \right| du. \tag{II-35}$$

Garber and Rozenvasser also note that in the practical use of the estimate, equation (II-20) should be transformed to

$$x = W_*(p) y_* + \phi_* \tag{II-36}$$

where

$$W_*(p) = \frac{W(p)}{1 + \lambda W(p)} \quad , \tag{II-37}$$

$$y_* = f(x) + \lambda x \quad , \tag{II-38}$$

and

$$\phi_* = \frac{\phi}{1 + \lambda W(p)} \quad . \tag{II-39}$$

The optimum value of λ, the linear rotation, is then chosen so as to minimize the estimate.

CHAPTER III

INVESTIGATION OF THE APPLICATION OF ESTIMATES TO FIRST ORDER SYSTEMS

Introduction

For a practical evaluation of the application of error estimates for the describing function method to any system, attention must be given to the practical range of operation and range of parameter values of the system. A basic part of the investigation, in this chapter and the next, is a determination of the usefulness of the error estimates as applied to what are considered practical first and second order systems.

The general nonlinear system considered is of the form indicated in Figure 1. The input to the system, r(t), is a sinusoid, Rsin wt, and the linear transfer function, G(s), is of the general form

$$G(s) = \frac{k}{s+a} \quad ; \qquad a, k \text{ real} \tag{III-1}$$

but can be gain normalized to the form

$$G(s) = \frac{1}{s+a} \tag{III-2}$$

without loss of generality.

The nonlinear function considered, f(e), is a unit saturation function as defined by equation (II-1). It is chosen because it represents a continuous odd symmetric nonlinearity, and a good approximation to many saturation type

nonlinearities existing in practical control systems. The fact that it is continuous and odd symmetric means that the most advanced form of the error estimates can be applied to the system.

Application of the describing function

The describing function for the unit saturation nonlinearity takes the form[1]

$$K_{eq}(E) = g(E) = \frac{1}{\pi}\left[2\theta_2 - \sin(2\theta_2)\right] + \frac{4}{\pi E}\cos(\theta_2) \qquad \text{(III-3)}$$

where

$$\theta_2 = \text{arc sin } (1/E) \; . \qquad \text{(III-4)}$$

This can be rewritten as

$$g(E) = \frac{2}{\pi}\left\{\text{arc sin } (1/E) + (1-1/E^2)^{\frac{1}{2}}/E\right\} . \qquad \text{(III-5)}$$

The magnitude relationship, equation (I-8), then becomes

$$\frac{E}{R} = \left|\frac{1}{1+g(E)G(jw)}\right| = \left|\frac{1}{1+g(E)/(wj+a)}\right| = \frac{a^2+w^2}{\left\{w^2 g(E)^2 + \left[a^2+w^2+ag(E)\right]^2\right\}^{\frac{1}{2}}} \qquad \text{(III-6)}$$

so that here equation (I-11) is written as

$$R = \frac{E}{a^2+w^2}\left\{w^2 g(E)^2 + \left[a^2+w^2+ag(E)\right]^2\right\}^{\frac{1}{2}} . \qquad \text{(III-7)}$$

The phase relationship of equation (I-9) becomes

$$\theta = \left\langle \frac{1}{1+g(E)G(jw)} = \arctan\left\{\frac{wg(E)}{w^2+a^2+ag(E)}\right\} . \right. \qquad \text{(III-8)}$$

---

[1] Gibson, op. cit., p. 364.

I. The Sandberg Estimate

Because the case where the input is a sinusoid and the nonlinearity odd symmetric is being considered, the final estimate form of equation (II-17) can be used together with Theorem IV. The estimate form of equation (II-14) was felt to be too unwieldy for practical use, and hence is not considered here.

It now becomes necessary to relate the Sandberg notation to the notation of the system of Figure 1. For $\psi = f(e)$, a unit saturation nonlinearity, α and β become

$$\alpha = 0 \quad ; \quad \beta = 2 \, . \tag{III-9}$$

The linear transfer function is identified as[2]

$$F(jw) = -G(jw) = \frac{-1}{jw + a} \, . \tag{III-10}$$

Then

$$\left| \frac{F(jw)}{1-F(jw)} \right| = \left| \frac{-1}{jw + a + 1} \right| = \frac{1}{\left\{ w^2 + (1+a)^2 \right\}^{\frac{1}{2}}} \, . \tag{III-11}$$

Equation (II-19) becomes, for this case,

$$q = \sup_{n \text{ odd}} \left\{ \frac{1}{\left[n^2 w^2 + (1+a)^2 \right]^{\frac{1}{2}}} \right\} = \frac{1}{\left\{ w^2 + (1+a)^2 \right\}^{\frac{1}{2}}} < 1 \, . \tag{III-12}$$

Now equations (III-11) and (III-12) can be identified as the

---

[2] It is noted that Sandberg considers a positive feedback system, while the system of Figure 1 has negative feedback. This accounts for the minus sign in equation (III-10).

M curve,[3] $|M(jw)|$, of the linear transfer function $G(jw) = 1/(jw+a)$. The crossover frequency,[4] w_c, of the linear transfer function $F(jw)$ is defined by the relationship

$$|F(jw_c)| = 1 = \frac{1}{\left\{w_c^2 + a^2\right\}^{\frac{1}{2}}} ; \qquad \text{(III-13)}$$

which implies

$$w_c^2 = 1 - a^2 ;$$

$$w_c = \left[1 - a^2\right]^{\frac{1}{2}} . \qquad \text{(III-14)}$$

Thus a crossover exists as long as $a < 1$. From a practical standpoint, a crossover would always exist for the linear transfer function. Moreover, stability considerations and practical realization normally dictates that $a \geq 0$. Therefore the range of the parameter a of practical interest is

$$0 \leq a < 1 . \qquad \text{(III-15)}$$

Under these conditions it can be seen that the q defined in equation (III-12) satisfies the key inequality of equation (III-12), namely $q < 1$, for all frequencies in the range $0 \leq w \leq \infty$. The normal frequency range of interest would be approximately the decade below w_c defined by

---

[3] John L. Bower and Peter M. Schultheiss, Introduction to the Design of Servomechanisms (New York: John Wiley and Sons, Inc., 1958), pp. 211-226.

[4] Bower and Schultheiss, op. cit., pp. 162-164.

$$\frac{w_c}{10} \leq w \leq w_c \quad . \tag{III-16}$$

Obviously, in this case the Sandberg estimate can be applied in the required frequency range. It is also apparent that

$$\sup_{n \in \mathcal{R}} \left| \frac{F_n}{1 - F_n} \right| = \frac{1}{\left\{9w^2 + (1+a)^2\right\}^{\frac{1}{2}}} \quad , \tag{III-17}$$

since the expression of equation (III-11) is monotonic decreasing with a. The norms $\|\hat{x} + y\|$ and $\|x - \hat{x}\|$ are readily identified as

$$\|\hat{x} + y\| = \|\hat{e}\| = \|E \sin(wt + \theta)\| = \frac{E}{\sqrt{2}} \tag{III-18}$$

and

$$\|x - \hat{x}\| = \|e - \hat{e}\| \tag{III-19}$$

respectively.

The final form of the estimate as given in equation (II-17) becomes

$$\|e - \hat{e}\| \leq \frac{\sqrt{2}\left[9w^2 + (1+a)^2\right]^{-\frac{1}{2}} E}{1 - \left\{w^2 + (1+a)^2\right\}^{-\frac{1}{2}}} \quad . \tag{III-20}$$

If the waveform $[e(t) - \hat{e}(t)]$ is assumed approximately sinusoidal then the rms norm of inequality (III-20) can be transformed to a magnitude norm inequality of the form

$$|e - \hat{e}| \leq \frac{2\left[9w^2 + (1+a)^2\right]^{-\frac{1}{2}} E}{1 - \left\{w^2 + (1+a)^2\right\}^{-\frac{1}{2}}} \quad . \tag{III-21}$$

This will then be consistent with the norm of Garber and Rozenvasser's estimate.

Numerical results of application of the Sandberg estimate are given at the end of this chapter.

II. The Garber-Rozenvasser Estimate

The linear transfer function of the Garber-Rozenvasser system (see Figure 3) becomes

$$W(p) = -G(p) = \frac{-1}{p+a} \quad . \tag{III-22}$$

The kernel, $\Phi(t-\tau)$, then is written as

$$\Phi(t-\tau) = \frac{-e^{-a(t-\tau)}}{1+e^{-aT/2}} \quad ; \quad 0 \leq t-\tau \leq T/2 \tag{III-23}$$

and the function I(w) of equation (II-32) becomes

$$I(w) = \frac{1}{a} \tanh\left[\frac{a\pi}{2w}\right] . \tag{III-24}$$

For the unit saturation nonlinearity, the uniform Lipschitz condition of equation (II-30) becomes

$$|f(\xi_1) - f(\xi_2)| \leq 1\cdot|\xi_1 - \xi_2| ; \tag{III-25}$$

so that

$$MI(w) = \frac{1}{a} \tanh\left[\frac{a\pi}{2w}\right] . \tag{III-26}$$

Then the condition for applicability of the estimate is

$$1 - \frac{1}{a} \tanh\left[\frac{a\pi}{2w}\right] > 0 , \tag{III-27}$$

or

$$\frac{1}{a} \times \tanh\left[\frac{a\pi}{2w}\right] < 1 . \tag{III-28}$$

It should be recalled that a is considered in the range $0 \leq a < 1$ so that the function $\tanh\left[\frac{a\pi}{2w}\right]/a$ is monotonic decreasing with increasing w, and always greater than 1 at $w = 0$. Thus the estimate cannot be applied in the complete range $0 \leq w \leq \infty$. If the function $\tanh\left[\frac{a\pi}{2w}\right]/a$ is evaluated

at $w = w_c$ the resulting expression is:

$$\tanh\left[\frac{a\pi}{2w_c}\right]\Big/a \;=\; \tanh\left[\frac{a\pi}{2\sqrt{1-a^2}}\right]\Big/a \;. \qquad \text{(III-29)}$$

This expression was evaluated for $0 \leq a \leq 1$ at .01 intervals and the minimum of 1 occurred at the upper limit $a = 1$. Thus, for all a in the region of interest, the inequality of equation (III-28) is not satisfied at the crossover frequency. Moreover, this means that the inequality (III-28) is not satisfied for all $w \leq w_c$ and, particularly, is not satisfied in the operating region $\frac{w_c}{10} \leq w \leq w_c$ defined as the practical range.

Application of linear rotation

The inapplicability of the Garber-Rozenvasser estimate in the region of interest for a first order system necessitates the use of the linear rotation concept in order to get any estimate, leave alone the optimum one. Application of the linear rotation concept produces a transformed system defined in equation (II-36), where in this case

$$W_*(p) \;=\; \frac{-1/(p+a)}{1-\lambda/(p+a)} = \frac{-1}{p+a-\lambda}\;, \qquad \text{(III-30)}$$

from equation (II-37).

Now for $W_*(p)$, the function I(w) will become

$$I_*(w) \;=\; \frac{1}{a-\lambda} \times \tanh\left[\frac{(a-\lambda)\pi}{2w}\right]. \qquad \text{(III-31)}$$

The new Lipschitz condition constant becomes

$$M_* = 1 + \lambda \quad ; \quad \lambda \geq 0$$
$$= 1 - |\lambda| \quad ; \quad -\frac{1}{2} \leq \lambda \leq 0$$
$$= |\lambda| \quad ; \quad -\infty \leq \lambda \leq -\frac{1}{2} \, . \tag{III-32}$$

Therefore, $M_*I_*(w)$ is written as

$$M_*I_*(w) = \frac{1 + \lambda}{a - \lambda} \tanh\left[\frac{(a - \lambda)\pi}{2w}\right] ; \quad \lambda > 0$$
$$= \frac{1 - |\lambda|}{a + |\lambda|} \tanh\left[\frac{(a + |\lambda|)\pi}{2w}\right] ; -\frac{1}{2} \leq \lambda \leq 0$$
$$= \frac{|\lambda|}{a + |\lambda|} \tanh\left[\frac{(a + |\lambda|)\pi}{2w}\right] ; -\infty \leq \lambda \leq -\frac{1}{2} \, . \tag{III-33}$$

It is obvious from the form of equation (III-33) that a value of λ can always be found so that $M_*I_* < 1$ for any a in the range $0 \leq a \leq 1$ and any w. Thus the linear rotation concept does make the Garber-Rozenvasser estimates applicable in the region of interest.

Approximation to max $|J_1(t)|$

The transformed system of equation (II-36) must be considered in the evaluation of $\max|J_1|$. Then the transformed nonlinearity [5] becomes

$$f_*(x) = f(x) + \lambda x \tag{III-34}$$

and the transformed input becomes

$$\phi_*(t) = \frac{p + a}{p + a - \lambda}\left[\phi(t)\right] \, , \tag{III-35}$$

---

[5] The transformed nonlinearity is also odd symmetric, so that the Garber-Rozenvasser estimate can still be applied.

where $(p+a) / (p+a-\lambda)$ is a linear operator operating on $\phi(t)$. The term $\max_{0\leq t\leq T/2} |J_1(t)|$ can be approximated for the transformed system as indicated by equation (II-35). The result is then

$$\max_{0\leq t\leq T/2} |J_1(t)| \leq \left\{ \max_{0\leq \tau\leq T/2} \left| f_* \left[x_{app}(\tau) \right] \right| \right\} \int_0^{T/2} |\Phi_*(u) - \Phi_{1*}(u)| \, du \tag{III-36}$$

where

$$\Phi_*(u) = \frac{-e^{-(a-\lambda)u}}{1+e^{-(a-\lambda)T/2}} \quad ; \tag{III-37}$$

and

$$\Phi_{1*}(u) = \frac{w}{\pi} \left[W_*(jw) e^{jwu} + W(-jw) e^{-jwu} \right]$$

$$= \frac{-4 \sin(wu+\alpha_1)}{T\left[(a-\lambda)^2 + w^2\right]^{\frac{1}{2}}} \quad , \tag{III-38}$$

where

$$\alpha_1 = \arctan \left[\frac{a-\lambda}{w} \right] \quad . \tag{III-39}$$

Now the term,

$$\max_{0\leq \tau\leq T/2} \left| f_* \left[x_{app}(\tau) \right] \right| = \max_{0\leq \tau\leq T/2} \left| f \left[E \sin(w\tau+\theta) \right] + \lambda E \sin(w\tau+\theta) \right| \, , \tag{III-40}$$

of equation (III-36) can be evaluated fairly easily for given λ and E. Also, the integral of equation (III-37) can be calculated on a digital computer quite readily. Through the use of a root finding subroutine, the zeros of $\left[\Phi_*(u) - \Phi_{1*}(u) \right]$ can be found in the interval $0 \leq u \leq T/2$, and the integrals easily calculated and summed for the intervals in which $\left[\Phi_*(u) - \Phi_{1*}(u) \right]$ does not change sign.

The details of evaluation are given in Appendix A.

Exact evaluation of $\max|J_1(t)|$

For a sinusoidal input the expression for $J_1(t)$ of equation (II-28) becomes

$$J_1(t) = \int_0^{T/2} \Phi_{h*}(t-\tau)\, f_*[x_{app}(\tau)]\, d\tau . \qquad \text{(III-41)}$$

This can be rewritten as

$$J_1(t) = \int_0^{T/2} \left[\Phi_*(t-\tau) - \Phi_{1*}(t-\tau)\right] f_*[x_{app}(\tau)]\, d\tau$$

$$= \int_0^{T/2} \Phi_*(t-\tau) f_*[x_{app}(\tau)]\, d\tau - \int_0^{T/2} \Phi_{1*}(t-\tau) f_*[x_{app}(\tau)]\, d\tau . \qquad \text{(III-42)}$$

However, consideration of equation (II-25) will yield

$$\int_0^{T/2} \Phi_{1*}(t-\tau) f_*[x_{app}(\tau)]\, d\tau = x_{app}(t) - \phi_{1*}(t) , \qquad \text{(III-43)}$$

so that

$$J_1(t) = \int_0^{T/2} \Phi_*(t-\tau) f_*[x_{app}(\tau)]\, d\tau + \phi_{1*}(t) - x_{app}(t) . \qquad \text{(III-44)}$$

The remaining integral of equation (III-44) can be evaluated exactly for t in the range $0 \leq t \leq T/2$. The details of the evaluation of $J_1(t)$ for the first order system are given in Appendix A along with the final expression for $J_1(t)$ (which is too complicated to present here). The exact* calculation of $\max_{0 \leq t \leq T/2} |J_1(t)|$ then involves using a digital computer to compute $|J_1(t)|$ at very small intervals in the range $0 \leq t \leq T/2$ and find the maximum value. A comparison is made at the end of this chapter between an exact evaluation of $\max|J_1|$ and an approximate one.

---

*i.e. to within computer accuracy.

Minimization of error estimate

With M_*I_* and $\max|J_1|$ known for any λ, the error estimate of equation (II-31) becomes, for given λ,

$$|x - x_{app}| = |e - \hat{e}| \leq \frac{\max|J_1|}{1 - M_*I_*} \quad . \qquad \text{(III-45)}$$

It is then a matter of finding the optimum value of λ, λ_{opt}, to minimize the estimate. In general the process of finding λ_{opt} can be very tedious, since λ_{opt} can depend on a, w, and even E for the first order case. The general procedure would then be to iterate λ over the applicable range for given a, w, and E to find the minimum estimate. It was felt that a simpler approach, although not necessarily one yielding λ_{opt}, might be to consider a minimization of M_*I_* rather than the complete error bound. This might even yield λ_{opt} if M_*I_* changed much more rapidly with λ than did $\max|J_1|$. Certainly a minimization of M_*I_* is valid in the sense that it would ensure that the Garber-Rozenvasser bound could be applied. An investigation of this approach is developed in Appendix A.

III. A Comparison Of Results

Some typical first order systems were considered and the various error estimates calculated. Analog simulation was employed for the systems considered in order to measure the actual maximum magnitude of error encountered in using the describing function approximation.

TABLE I

FIRST ORDER ERROR ESTIMATES

	w radians per sec.	E	ERROR ESTIMATES			
			Sandberg	G-R1	G-R2	Measured
System 1	$\frac{w_c}{2}$: .4999	1.5	13.82	4.68	1.11	.07
a = .02	w_c: .9998	1.5	3.16	.75	.18	.02
w_c = .9998	$\frac{w_c}{2}$: .4999	5.0	46.08	14.05	3.57	.24
	w_c: .9998	5.0	10.53	2.26	.57	.03
System 2	$\frac{w_c}{2}$: .4994	1.5	11.72	3.47	.82	.08
a = .05	w_c: .9987	1.5	3.05	.73	.17	.01
w_c = .9987	$\frac{w_c}{2}$: .4994	5.0	39.06	10.42	2.64	.22
	w_c: .9987	5.0	10.16	2.18	.56	.03
System 3	$\frac{w_c}{2}$: .4975	1.5	9.42	2.48	.59	.08
a = .1	w_c: .9950	1.5	2.89	.69	.16	.02
w_c = .995	$\frac{w_c}{2}$: .4975	5.0	31.42	7.44	1.89	.22
	w_c: .9950	5.0	9.65	2.07	.53	.02

The method of measurement in the analog experiments was quite simple, but was considered accurate enough compared to the numbers calculated for the various bounds. The measurement technique was to use a transfer function analyzer to measure the amplitude and phase of the fundamental of the input to the nonlinearity. The absolute value of the maximum difference between the measured sinusoid and the describing function approximation would then yield the measured bound. The assumption in this method is that the actual input to the nonlinearity closely approximates a sinusoid. This assumption seemed to be valid for all cases tried.

Table I gives calculated and measured error estimates for three different first order systems at two frequencies and two saturation levels. The most significant result is the fact that the calculated error estimates exceed the measured ones by factors of 7 up to 400. While the second decimal place of the measured estimates is likely in error, the huge discrepancy between calculated and measured estimates is still apparent. A comparison of the various estimates indicates that the Sandberg estimate exceeds the Garber-Rozenvasser with the approximation to $\max|J_1|$ (G-R1) by a factor between 3 and 4.5. Similarly, the Garber-Rozenvasser estimate with approximate $\max|J_1|$ exceeds the Garber-Rozenvasser estimate with exact $\max|J_1|$ (G-R2) by a

FIGURE 4

$Q=.01, \omega_c=1, E=1.5$

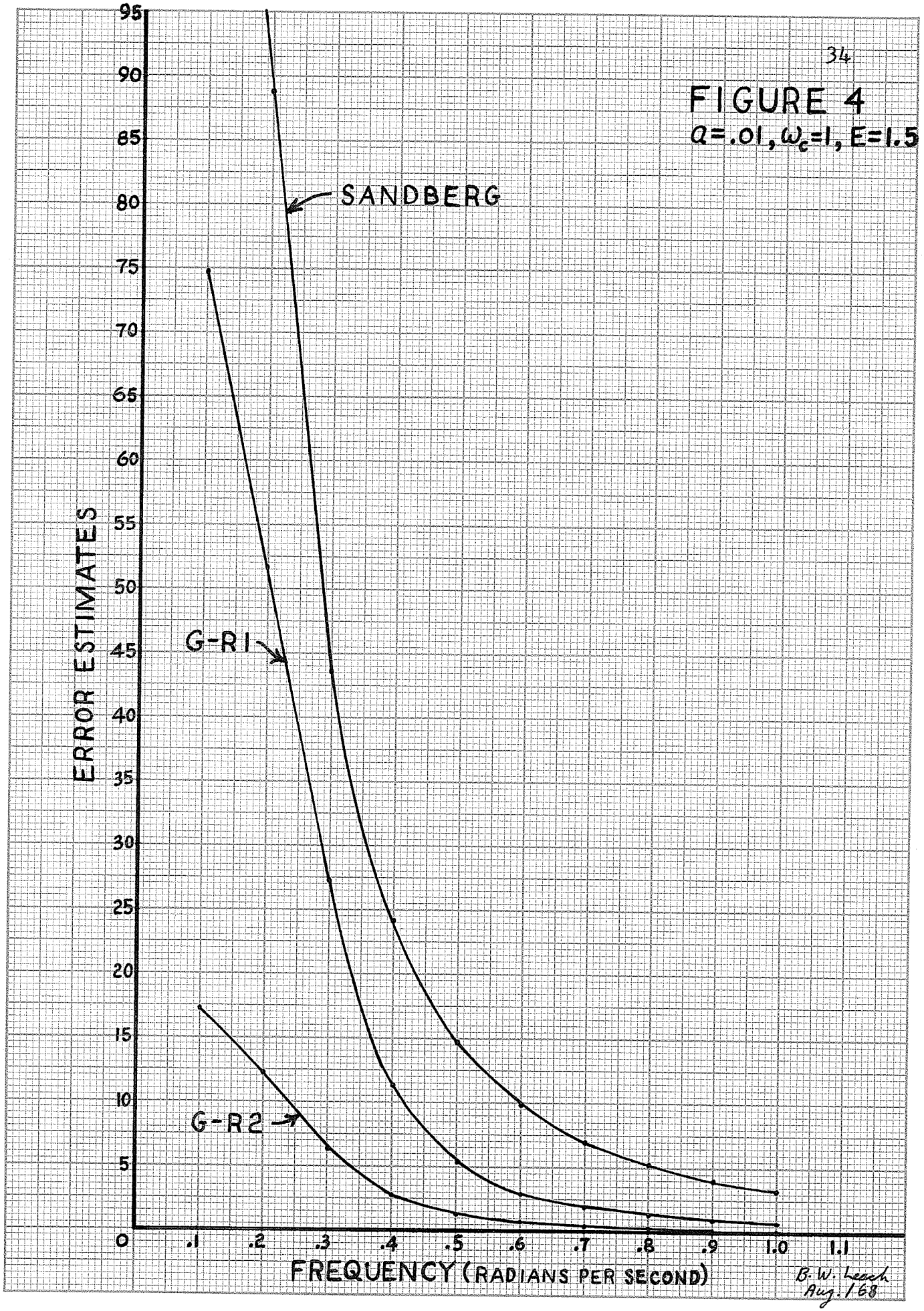

B. W. Leach
Aug. 1968

factor of about 4. Finally, the Garber-Rozenvasser estimate with exact $\max|J_1|$ exceeds the measured results by a factor between 7 and 20.

Figure 4 gives a graphical comparison of the three calculated error estimates over the frequency range $w_c/10 \leq w \leq w_c$. The improvement in going from Sandberg to G-R1 to G-R2 is clearly indicated. This graph also shows the typical decrease with frequency of the calculated estimates indicating the expected improved filtering of the linear part of the system as frequency is increased.

CHAPTER IV

INVESTIGATION OF THE APPLICATION OF ESTIMATES TO SECOND ORDER SYSTEMS

The system

The only change to be made in the system from that of the previous chapter is in the linear transfer function. The system is still of the general form of Figure 1 with a sinusoidal input, $r(t) = R \sin wt$, and a unit saturation nonlinearity. The linear transfer function, $G(s)$, is assumed to be of the general form

$$G(s) = \frac{k}{(s+a)(s+b)} \quad ; \; a, \; b, \; k \text{ real} \qquad \text{(IV-1)}$$

but normalization with respect to b will yield

$$G(s) = \frac{k}{(s+a)(s+1)} \quad , \quad a < 1 \qquad \text{(IV-2)}$$

as a general transfer function which can be considered.

Application of the describing function

The describing function, $g(E)$, for a unit saturation nonlinearity has already been expressed in equations (III-3), (III-4), and (III-5). The magnitude relation of equation (I-8) becomes, for the second order case,

$$E/R = \left| \frac{1}{1 + \frac{kg}{(jw+a)(jw+1)}} \right|$$

$$= \frac{w^2(1+a)^2 + (w^2 - a)^2}{\left\{k^2w^2g^2(1+a)^2 + \left[w^2(1+a)^2 - (a - w^2 + gk)(w^2 - a)\right]^2\right\}^{\frac{1}{2}}} \cdot \qquad \text{(IV-3)}$$

The phase relationship of equation (I-9) then becomes

$$\theta = \angle \frac{1}{1+gG(jw)} = \arctan \left\{ \frac{wk(1+a)g}{w^4+w^2(1+a^2)+a^2+gk(a-w^2)} \right\} . \tag{IV-4}$$

I. The Sandberg Estimate

The linear transfer function, in Sandberg's notation, becomes

$$F(jw) = -G(jw) = \frac{-k}{(jw+a)(jw+1)} . \tag{IV-5}$$

Thus

$$\left| \frac{F(jw)}{1 - F(jw)} \right| = \frac{k}{\left\{ (a+k-w^2)^2 + w^2(1+a)^2 \right\}^{\frac{1}{2}}} , \tag{IV-6}$$

and

$$q = \sup_{n \text{ odd}} \left\{ \frac{k}{\left[(a+k-n^2w^2)^2 + n^2w^2(1+a)^2 \right]^{\frac{1}{2}}} \right\} . \tag{IV-7}$$

Equation (IV-6) is the M curve, $|M(jw)|$, of the linear transfer function G(jw). Normally, for second order systems a resonance peak is associated with the M curve at the resonant frequency w_r. Here w_r would be defined as

$$w_r = \left[a + k - \frac{(1+a)^2}{2} \right]^{\frac{1}{2}} , \tag{IV-8}$$

under the condition

$$2k > 1+a^2 .$$

Also, the crossover frequency, w_c, of this system would be

$$w_c = \left\{ -\frac{(1+a^2)}{2} + \left[\frac{(1+a^2)^2}{4} + k^2 - a^2 \right]^{\frac{1}{2}} \right\}^{\frac{1}{2}}, \qquad \text{(IV-10)}$$

subject to the condition

$$k > a. \qquad \text{(IV-11)}$$

Hence inequalities (IV-9) and (IV-11) would be satisfied for practical systems. Moreover, a resonance peak, $|M(jw_r)|$, greater than 1 is also desired in a practical system to ensure reasonably fast response. In most cases w_r and w_c are fairly close in value so that the frequency region of operation of the system is normally below w_r. If $w_1 \leq w \leq w_2$ defines the region in which

$$|M(jw)| = \left| \frac{F(jw)}{1 - F(jw)} \right| \geq 1, \qquad \text{(IV-12)}$$

then it becomes apparent that, for a driving frequency $w_0 < w_r$, there can easily exist a value of n such that $w_1 \leq nw_0 \leq w_2$. If this is the case then the condition of applicability of the estimate, $q < 1$, does not hold.

Obviously, as the system becomes more resonant the likelihood that the condition of applicability holds tends to decrease. Similarily, if the system becomes less resonant then the condition of applicability has a better chance of holding.

II. The Garber-Rozenvasser Estimate

The linear transfer function of the Garber-Rozenvasser system is now written as

$$W(p) = -G(p) = \frac{-k}{(p+a)(p+1)} , \qquad \text{(IV-13)}$$

and the kernel, $\Phi(t-\tau)$, becomes

$$\Phi(t-\tau) = \frac{-k}{1-a}\left[\frac{e^{-a(t-\tau)}}{1+e^{-aT/2}} - \frac{e^{-(t-\tau)}}{1+e^{-T/2}}\right]; \quad 0 \leq t-\tau \leq T/2 \qquad \text{(IV-14a)}$$

$$= \frac{k}{1-a}\left[\frac{e^{-aT/2}\,e^{-a(t-\tau)}}{1+e^{-aT/2}} - \frac{e^{-T/2}\,e^{-(t-\tau)}}{1+e^{-T/2}}\right]; \quad 0 \leq \tau - t \leq T/2 \qquad \text{(IV-14b)}$$

The function I(w) becomes

$$I(w) = \frac{k}{1-a}\left\{\frac{1+e^{-T/2}\,-2e^{-u^*}}{1+e^{-T/2}} - \frac{\left[1+e^{-aT/2}\,-2e^{-au^*}\right]}{a\left(1+e^{-aT/2}\right)}\right\}, \qquad \text{(IV-15)}$$

where

$$u^* = \frac{1}{1-a}\ln\left[\left(1+e^{-aT/2}\right) / \left(1+e^{-T/2}\right)\right]. \qquad \text{(IV-16)}$$

The condition for applicability of the estimate is then

$$I(w) = \frac{k}{1-a}\left\{\frac{1+e^{-T/2}\,-2e^{-u^*}}{1+e^{-T/2}} - \frac{1+e^{-aT/2}\,-2e^{-au^*}}{a\left(1+e^{-aT/2}\right)}\right\} < 1. \qquad \text{(IV-17)}$$

In order to investigate the condition of applicability, values of $I(w_c)$ were determined for systems in a parameter grid defined by $0 \leq a \leq 1$ and $1 \leq k \leq 100$. The minimum of $I(w_c)$ was found, and turned out to be 1.01. While not conclusive, this investigation seemed to suggest that, for the practical range of system parameter values

and for $w \leq w_c$, the condition of applicability of the Garber-Rozenvasser estimate would not hold. It should be noted that the function I(w) was found to be a monotonic decreasing function of w, so that the foregoing conclusion would at least be valid for the particular values of a and k tested.

Application of linear rotation

Once again the linear rotation concept must be applied in order to try to make the Garber-Rozenvasser estimate applicable in the region $w_c/10 \leq w \leq w_c$, as well as to minimize the estimate. When the linear rotation concept is applied, the linear transfer function of the transformed system becomes

$$W_*(p) = \frac{-k/[(p+a)(p+1)]}{1 - \lambda k/[(p+a)(p+1)]} = \frac{-k}{p^2+(1+a)p+a-\lambda k} . \qquad \text{(IV-18)}$$

This can be written as

$$W_*(p) = \frac{-k}{(p-p_1)(p-p_2)} , \qquad \text{(IV-19)}$$

where

$$p_1 = \frac{-(1+a)}{2} + \frac{[4\lambda k + (1-a)^2]^{\frac{1}{2}}}{2} ; \qquad \text{(IV-20a)}$$

$$p_2 = \frac{-(1+a)}{2} - \frac{[4\lambda k + (1-a)^2]^{\frac{1}{2}}}{2} . \qquad \text{(IV-20b)}$$

Two cases can be considered, depending on the value of λ. If the condition,

$$\lambda > \frac{-(1-a)^2}{4k} , \qquad \text{(IV-21)}$$

holds, then p_1 and p_2 are real, and the function $I_*(w)$ can be found in exactly the same manner as I(w) of equation (IV-15). The result is

$$I_*(w) = \frac{k}{p_1 - p_2}\left\{\frac{1+e^{p_2T/2}-2e^{p_2u^*}}{-p_2(1+e^{p_2T/2})} - \frac{1+e^{p_1T/2}-2e^{p_1u^*}}{-p_1(1+e^{p_1T/2})}\right\}, \tag{IV-22}$$

where

$$u^* = \frac{1}{p_1 - p_2}\ln\left[(1+e^{p_1T/2}) / (1+e^{p_2T/2})\right]. \tag{IV-23}$$

However, if the condition,

$$\lambda < -\frac{(1-a)^2}{4k}, \tag{IV-24}$$

holds, then p_1 and p_2 are complex conjugates of the form

$$p_1 = -A + Bj \quad ; \quad p_2 = -A - Bj, \tag{IV-25}$$

where

$$A = \frac{(1+a)}{2} \quad ; \quad B = \frac{\left[-4\lambda k - (1-a)^2\right]^{\frac{1}{2}}}{2}. \tag{IV-26}$$

The kernel, $\Phi_*(u)$, is then written as

$$\Phi_*(u) = \frac{ke^{-Au}\left\{e^{-AT/2}\sin(BT/2)\cos(Bu) - \left[1+e^{-AT/2}\times\cos(BT/2)\right]\sin(Bu)\right\}}{B\left\{1+2e^{-AT/2}\times\cos(BT/2)+e^{-AT}\right\}} \quad ; \; 0 \leq u \leq T/2, \tag{IV-27}$$

or more succinctly as

$$\Phi_*(u) = \frac{ke^{-Au}\sin(Bu+\gamma)}{B\left\{1+2e^{-AT/2}\times\cos(BT/2)+e^{-AT}\right\}^{\frac{1}{2}}}; \tag{IV-28}$$

where

$$\gamma = - \arctan \left\{ \frac{e^{-AT/2} \sin(BT/2)}{1 + e^{-AT/2} \times \cos(BT/2)} \right\} + \pi \ . \qquad \text{(IV-29)}$$

The zeros of $\Phi_*(u)$ in the interval $0 \leq u \leq T/2$ are the set $\{u_n\}$ defined by

$$\begin{aligned} u_1 &= \frac{\pi - \gamma}{B} \quad ; \quad \pi - \gamma > 0 \\ &= \frac{2\pi - \gamma}{B} \quad ; \quad \pi - \gamma < 0 \\ &\ \ \vdots \qquad\qquad \vdots \\ u_n &= \frac{n\pi - \gamma}{B} \quad ; \quad \pi - \gamma > 0 \ \text{ and } \ u_n \leq T/2 \\ &= \frac{(n+1)\pi - \gamma}{B} ; \quad \pi - \gamma < 0 \ \text{ and } \ u_n \leq T/2 \ . \end{aligned} \qquad \text{(IV-30)}$$

Once the zeros of $\Phi_*(u)$ are known in $0 \leq u \leq T/2$ then $I_*(w)$ can be expressed as

$$I_*(w) = \sum_{i=0}^{n} \int_{u_i}^{u_{i+1}} \left| \Phi_*(u) \right| du \ , \qquad \text{(IV-31)}$$

where $u_o = 0 \quad ; \quad u_{n+1} = T/2 \ .$ (IV-32)

The integral from one zero to the next is then a standard tabulated integral (in this case const $\times \int e^{-Au} \sin(Bu + \gamma) du$), and can be calculated rather simply.

The Lipschitz condition constant, M_*, remains the same as that given by equation (III-32), so that $M_* I_*(w)$ is now defined for all λ, but in a rather complicated manner.

Approximation to $\max|J_1(t)|$

The transformed nonlinearity, $f_*(x)$, remains as in equation (III-34). The transformed input, $\phi_*(t)$, becomes

$$\phi_*(t) = \frac{(p+a)(p+1)}{(p+a)(p+1)-\lambda k}\left[\phi(t)\right]. \qquad \text{(IV-33)}$$

In a manner similar to that employed in Chapter III, $\max_{0\leq t\leq T/2}|J_1(t)|$ can be approximated for given λ. The result is derived from the general expression of equation (III-36). For λ satisfying inequality (IV-21), the kernel, $\Phi_*(u)$, becomes

$$\Phi_*(u) = \frac{-k}{p_1-p_2}\left\{\frac{e^{p_1 u}}{1+e^{p_1 T/2}} - \frac{e^{p_2 u}}{1+e^{p_2 T/2}}\right\}, \qquad \text{(IV-34)}$$

where p_1 and p_2 are as given in equations (IV-12a) and (IV-12b). The fundamental approximation to the kernel, $\Phi_{1*}(u)$, is written as

$$\Phi_{1*}(u) = \frac{-4k\sin(wu+\sigma)}{T\left\{(p_1p_2-w^2)^2+w^2(p_1+p_2)^2\right\}^{\frac{1}{2}}}, \qquad \text{(IV-35)}$$

where

$$\sigma = \arctan\left[\frac{p_1p_2-w^2}{-(p_1+p_2)w}\right]. \qquad \text{(IV-36)}$$

When λ satisfies inequality (IV-24), then $\Phi_*(u)$ is as given in equation (IV-28), and $\Phi_{1*}(u)$ becomes

$$\Phi_{1*}(u) = \frac{-4k\sin(wu+\sigma_1)}{T\left\{(A^2+B^2-w^2)^2+4A^2w^2\right\}^{\frac{1}{2}}}; \qquad \text{(IV-37)}$$

where

$$\sigma_1 = \arctan\left[\frac{A^2+B^2-w^2}{2Aw}\right], \qquad \text{(IV-38)}$$

and A and B are as given in equation (IV-26). With $\Phi_*(u)$ and $\Phi_{1*}(u)$ known, the integral of equation (III-36) can be found by again using a root finding procedure on $\left[\Phi_*(u) - \Phi_{1*}(u)\right]$, and determining the integrals between the zeros. The details of evaluation are omitted, since they closely parallel those given in Appendix A for the first order case.

Exact evaluation of $\max|J_1(t)|$

The expression, $\max_{0\leq t\leq T/2}|J_1(t)|$, could be evaluated exactly, in a manner similar to what was done for the first order case. Because the details of evaluation would be much more complicated than those for the first order case, it was felt that an investigation of the approximation to $|J_1(t)|$ should be made first. The results of this investigation (together with the known improvement from an exact evaluation of $|J_1(t)|$ for the first order case) would indicate whether or not the amount of work involved in an exact evaluation would be justified.

Minimization of error estimate

A general method of minimizing the error estimate would involve an iteration of λ over a suitable range through the use of a digital computer. As in the first order case, it was thought that perhaps a minimization of M_*I_* would also yield the minimum bound or something close

to it. Also, it was felt that the first point of investigation should be the evaluation of $\min_{\lambda}\{M_* I_*\}$ because, if it turned out that $\min_{\lambda}\{M_* I_*\} \geq 1$ in all cases, then there would be no point in pursuing the investigation for the second order case. The evaluation of $\min_{\lambda}\{M_* I_*\}$ would also have to be done on a digital computer, since the expression for $M_* I_*$ is too complicated for analytical procedures. The results of this investigation are detailed in Appendix B.

III. Numerical Results

Correlation of resonance with applicability of the estimates

For the Sandberg estimate, it is quite obvious that the degree of resonance of the linear part of the system (as defined by M_p[1], the M peak) determines whether or not the estimate can be applied. In cases where the M peak is much greater than 1 it is very unlikely that the inequality $q < 1$ (see equation II-19) will be satisfied.

As a check to see how applicability of the Sandberg estimate is related to resonance for a typical second order system, M peak was varied from 1.155 down to .9 and the applicability of the Sandberg bound was tested in the range $\frac{w_c}{10} \leq w \leq w_c$ at $\frac{w_c}{10}$ intervals. The M peak was varied by taking a system with $k = 1$ and varying a from 0 to .20. The results showed that the bound could not be applied at any of the ten frequencies tested until $M_p = 1.069$, where the bound applied only at $.4w_c$. The bound could be applied

---

[1] $M_p = |M(jw_r)|$.

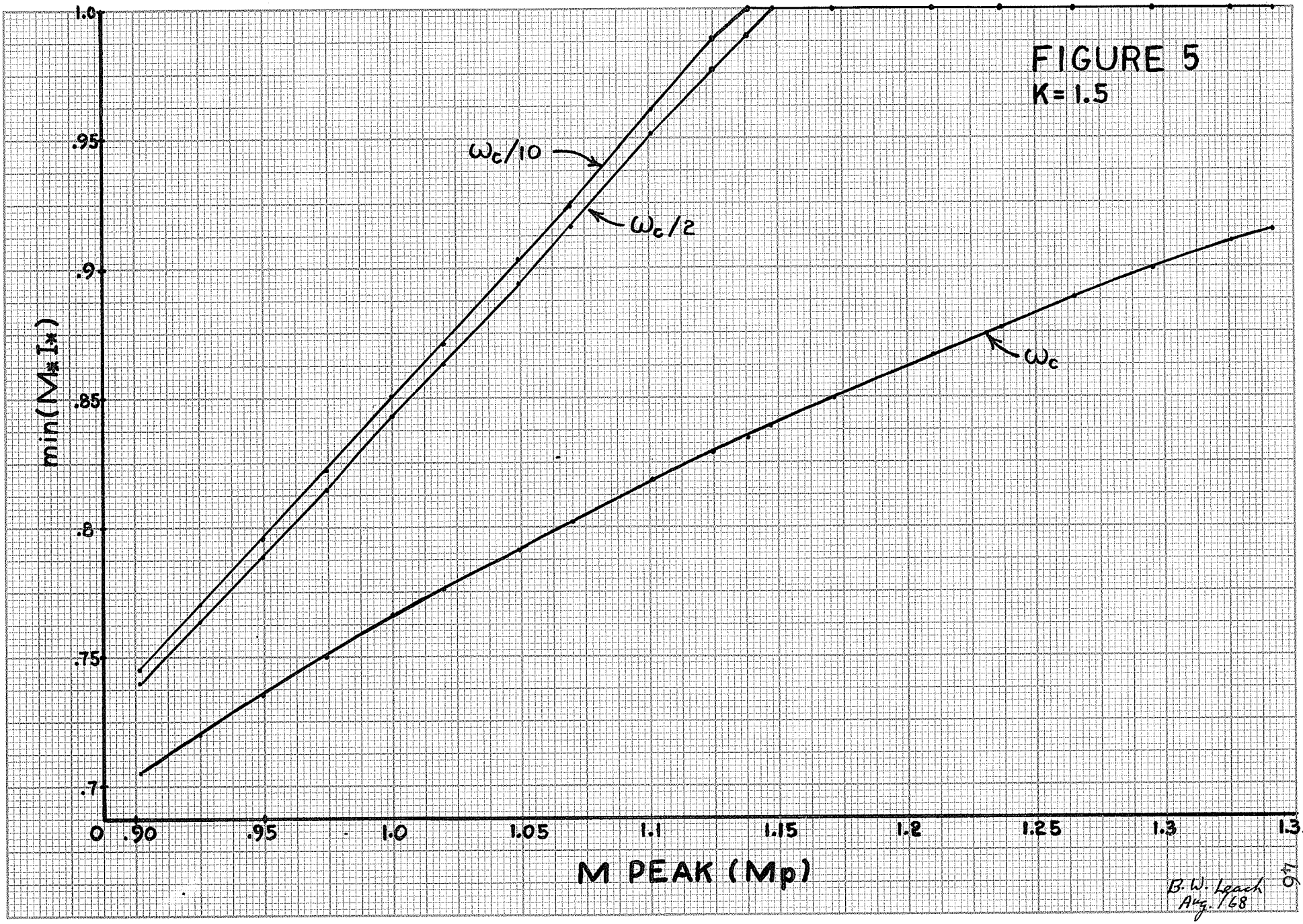
FIGURE 5
K = 1.5
$\omega_c/10$
$\omega_c/2$
ω_c
min(M*I*)
1.0
.95
.9
.85
.8
.75
.7
0
.90
.95
1.0
1.05
1.1
1.15
1.2
1.25
1.3
1.35
M PEAK (Mp)
B. W. Leach
Aug. 1968

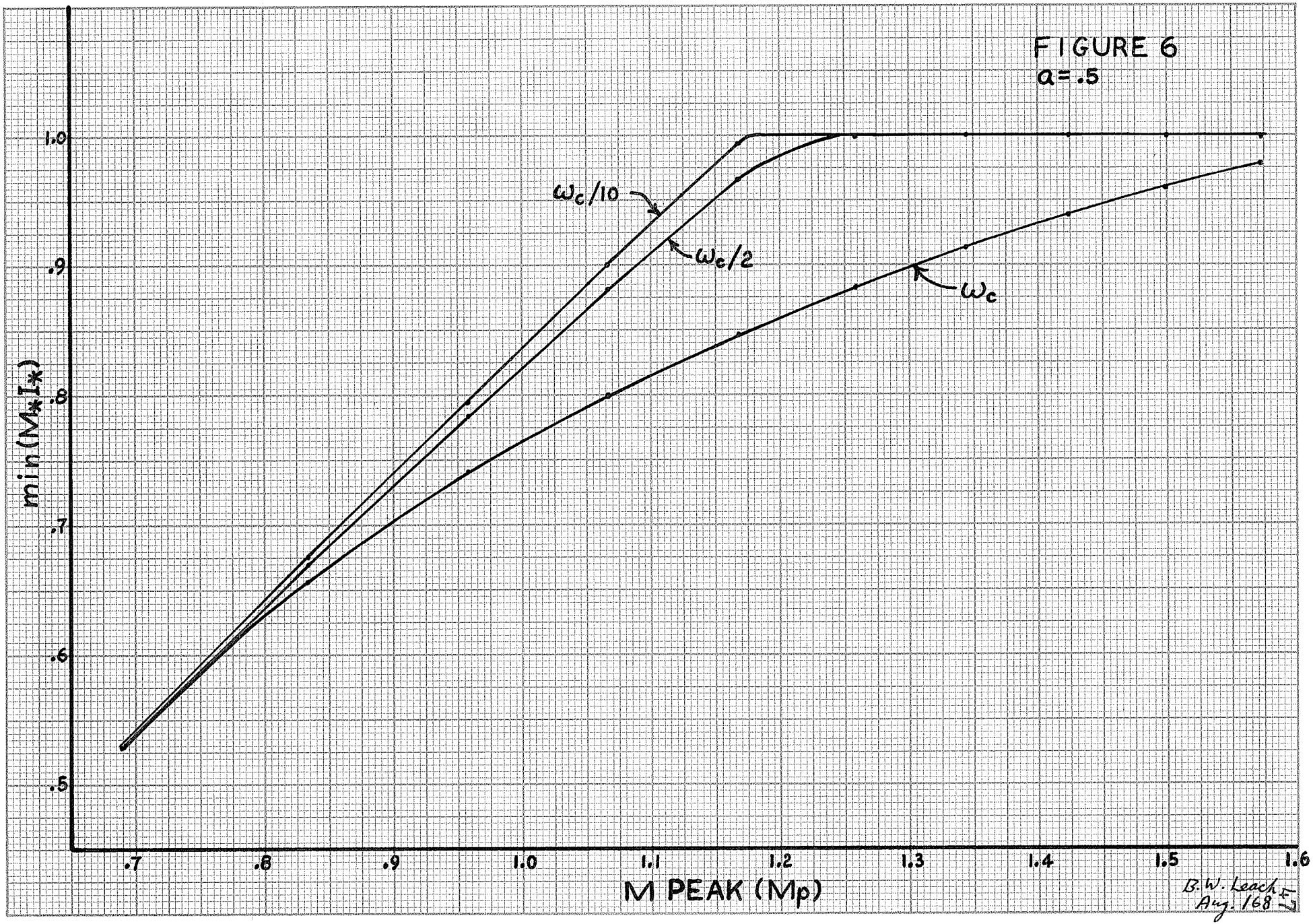

over about half the range only when M_p came down to 1.01. Finally, the bound became applicable over the whole range only for M_p less than 1.

The results of Appendix B seemed to indicate that there was a similar correlation between resonance and applicability of the Garber-Rozenvasser estimate. To investigate this, $\min_{\lambda} \{M_* I_*\}$ was plotted versus M_p at the frequencies $\frac{w_c}{10}$, $\frac{w_c}{2}$, and w_c. M_p was varied by taking a system with $k = 1.5$ and varying a over the range $0 \rightarrow .4$ so that M_p varied through the range $1.35 \rightarrow .9$. The results, plotted in Figure 5, indicate that $\min\{M_* I_*\}$ is monotonic increasing with M_p (for $\min\{M_* I_*\} < 1$) at all three frequencies. Furthermore, for $M_p = 1.15$ the Garber-Rozenvasser estimate can only be applied over about half the frequency range of interest. As M_p increases above 1.15, the range of application of the bound decreases below one half.

A further graph was made of $\min\{M_* I_*\}$ versus M_p, this time for a system in which a remained fixed at a value of .5 and k varied over the range $1 \rightarrow 5.5$. Figure 6 shows the plots, which are quite similar to those of Figure 5. It is noted, however, that for the case of Figure 6 it takes an M_p of 1.25 before the Garber-Rozenvasser estimate can only be applied over half the frequency range of interest. Figures 5 and 6 seem to suggest a monotonic increase of $\min\{M_* I_*\}$ with M_p (as long as $\min\{M_* I_*\}$ is less than one).

TABLE II

SECOND ORDER ERROR ESTIMATES

	w radians per sec.	E	ERROR ESTIMATES		
			Sandberg	G-R	Measured
System 1	$\frac{w_c}{2}$: .300	1.5	NA	35.75	.07
k = .7	w_c: .600	1.5	NA	.61	.02
a = .01	$\frac{w_c}{2}$: .300	5.0	NA	107.26	.13
w_c = .600	w_c: .600	5.0	NA	1.84	.03
M_p = 1.0275					
System 2	$\frac{w_c}{2}$: .2998	1.5	196.07	7.39	.03
k = .7	w_c: .5996	1.5	24.04	.57	.01
a = .03	$\frac{w_c}{2}$: .2998	5.0	653.56	22.18	.10
w_c = .5996	w_c: .5996	5.0	80.12	1.71	.02
M_p = .9969					
System 3	$\frac{w_c}{2}$: .5056	1.5	25.21	2.45	.14
k = 1.5	w_c: 1.0112	1.5	30.06	.44	.02
a = .3	$\frac{w_c}{2}$: .5056	5.0	84.06	7.34	.15
w_c = 1.0112	w_c: 1.0112	5.0	100.18	1.33	.07
M_p = .9831					

They also seem to indicate that if the M peak of the system is from 1.15 to 1.25 or greater, then the Garber-Rozenvasser estimate is likely to be applicable over less than half of the frequency range $\frac{w_c}{10} \leq w \leq w_c$.

Comparison of error estimates

Error estimates were calculated for cases in which the Garber-Rozenvasser and/or Sandberg error estimates could be applied. This necessitated investigating low resonance systems which are not considered too practical. A practical second order system would probably have an M peak of 1.2-1.4 in order to ensure reasonably fast response. Systems considered for the estimate comparisons had to have M peaks of one or less in order to ensure that both the Sandberg and Garber-Rozenvasser estimates could be applied.

Analog simulation was used for the systems considered in the estimate comparison so that actual maximum magnitudes of error involved in using the describing function could be compared to the estimates of the error. The measurement technique used was the same as the one described in Chapter III. Table II gives calculated and measured error estimates for three different second order systems at two frequencies and two saturation levels. The Garber-Rozenvasser estimate for approximate $\max|J_1|$ (G-R) is seen to be a substantial improvement over the Sandberg estimate. In some cases the Sandberg estimate exceeds the Garber-Rozenvasser one by

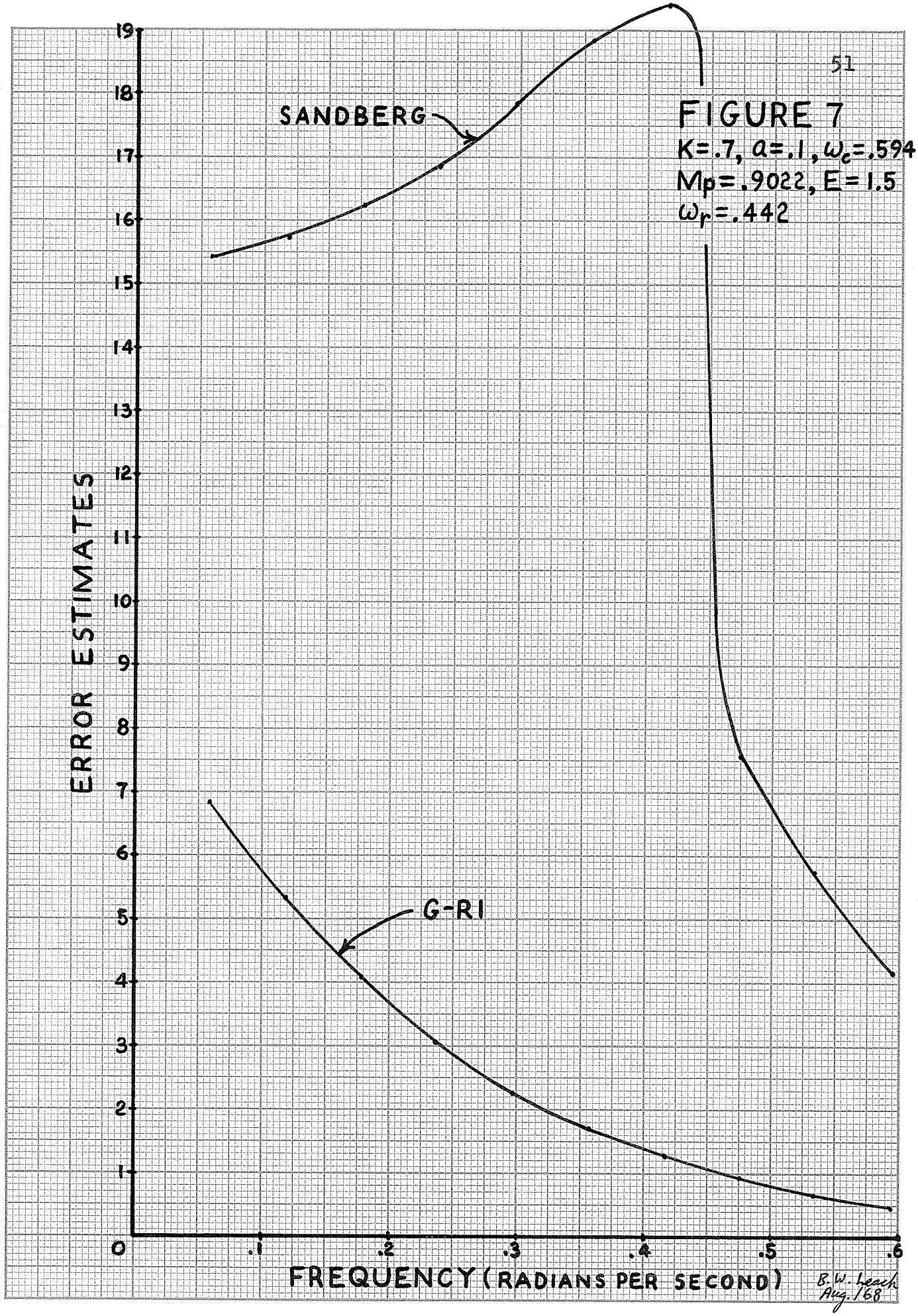

FIGURE 7

$K=.7,\ a=.1,\ \omega_c=.594$

$Mp=.9022,\ E=1.5$

$\omega_r=.442$

B. W. Leach
Aug. '68

factors as high as 75. For system 1, the Garber-Rozenvasser estimate yields a result where the Sandberg estimate fails. Nevertheless, the Garber-Rozenvasser estimate still exceeds the measured estimate by factors as high as 800! If the first order results are indicative, then an improvement by a factor of four or five can be expected by using the Garber-Rozenvasser estimate with exact $\max|J_1|$. It was felt that this improvement would not be substantial enough to warrant the amount of work involved in an exact calculation of $\max|J_1|$.

Figure 7 shows a graph of the Sandberg and Garber-Rosenvasser estimates versus frequency for a typical system. An interesting observation is that, while the Garber-Rosenvasser estimate is monotonic decreasing with frequency, the Sandberg estimate experiences a resonant peak at the resonant frequency of the linear part of the system. This is due to the direct relationship between the M curve and the error estimate.

CHAPTER V

CONCLUSIONS AND RECOMMENDATIONS FOR FUTURE WORK

For the first and second order systems studied, it was found that the Sandberg and Garber-Rozenvasser estimates were really of little or no use to a practical designer. In the first order case, both bounds could be applied, but the estimates were much too liberal to be of practical value. The Sandberg estimate was found to be the easiest to apply, but yielded the most liberal bound. The Garber-Rozenvasser estimate with the approximation to $\max|J_1|$ became more complicated to apply, but reduced the liberality of the estimate substantially. Finally, the Garber-Rozenvasser estimate with exact $\max|J_1|$ was the most difficult to apply, but gave the best estimate.

In the second order case it was found that the degree of resonance of the linear part of the system determined whether or not the estimates could be applied at all. It was found that, as the M peak increased, the range of applicability (within the frequency region of interest) of the error estimates decreased. The Garber-Rozenvasser estimate was found to apply over a slightly wider range of M peak values than did the Sandberg estimate. Also, for the cases in which the estimates could be applied, the Garber-Rozenvasser estimate with the approximation to $\max|J_1|$ was

found to be much better than the Sandberg estimate, but more difficult to apply. Even with the added improvement of an exact calculation of $\max|J_1|$ (as projected from the first order case) it was obvious that the Garber-Rozenvasser estimate would still be too liberal for practical purposes, and the complications of an exact calculation of $\max|J_1|$ would not be justified.

Some interesting findings were noted in the application of linear rotation to the Garber-Rozenvasser estimate. First of all, for both first and second order cases it was found that linear rotation had to be used if the estimate was to be applied in the region of interest. Secondly, a minimization of M_*I_* always produced the minimum estimate and λopt was always -.5. This meant that the bound was minimum for the minimum slope condition on $f_*[x]$. These observations made the job of applying the linear rotation much easier than first thought.

It should be noted that, although only a unit saturation nonlinearity was considered, most of the conclusions will hold regardless of the type of nonlinearity. The major pitfalls of both the Sandberg and Garber-Rozenvasser estimates are seen to be related to the linear transfer function and not to the nonlinearity. This is possibly the main weakness of the methods - the details of the nonlinearity

are overlooked, and only some type of slope condition is used to describe the nonlinearity. Perhaps future work should be devoted to a more thorough consideration of the nonlinearity. For example, in the case of the Garber-Rozenvasser estimate, a more exact calculation of the term J_2 (see equations II-27 and II-29) should lead to a better estimate. This would involve a detailed analysis of the nonlinearity, as was done for the exact calculation of J_1.

A further possibility for future work lies in the Sandberg bound expression of equation (II-14). This is an infinite series expression involving the Fourier coefficients of the higher harmonics of the approximate (describing function) output of the nonlinearity. Perhaps a finite series will give an adequate error estimate that can be of practical importance.

BIBLIOGRAPHY

(1) Bower, John L., and Peter M. Schultheiss, Introduction to the Design of Servomechanisms. New York: John Wiley and Sons, Inc., 1958. 510 pp.

(2) Garber, E. D., "Error Estimation in the Describing Function Method", Automation and Remote Control, Vol. 24, 1963, pp. 449-458.

(3) Garber, E. D., and E. N. Rozenvasser, "The Investigation of Periodic Regimes of Nonlinear Systems on the Basis of the Filter Hypothesis", Automation and Remote Control, Vol. 26, 1965, pp. 274-285.

(4) Gibson, John E., Nonlinear Automatic Control. New York: McGraw-Hill Book Company, Inc., 1963. 585 pp.

(5) Gille, J-C, M. J. Pelegrin, and P. Decaulne, Feedback Control Systems. New York: McGraw-Hill Book Company, Inc., 1959. 793 pp.

(6) Graham, Dunstan, and Duane McRuer, Analysis of Nonlinear Control Systems. New York: John Wiley and Sons, Inc., 1961. 482 pp.

(7) Holtzman, J. M., "Contraction Maps and Equivalent Linearization", The Bell System Technical Journal, Vol. XLVI, No. 10, December 1967, pp. 2405-2435.

(8) Johnson, E. C., "Sinusoidal Analysis of Feedback-Control Systems Containing Nonlinear Elements", Trans. AIEE, Vol. 71, Part II. Applications and Industry, July 1952, pp. 169-181.

(9) Korovkin, P. P., Linear Operators and Approximation Theory. Delhi: Hindustan Publishing Corp. (India), 1960. 338 pp.

(10) Liverman, T. P. G., Generalized Functions and Direct Operational Methods, Englewood Cliffs: Prentice-Hall, Inc., 1964. 338 pp.

(11) Mikusinski, Jan, Operational Calculus, New York: Pergamon Press, Inc., 1959. 495 pp.

(12) Moretti, Gino, Functions of a Complex Variable, Englewood Cliffs: Prentice-Hall, Inc., 1964. 456 pp.

(13) Rozenvasser, E. N., "On the Accurate Determination of Periodic Regimes in Sectionally Linear Automatic Control Systems", Automation and Remote Control, Vol. 21, 1960, pp. 902-910.

(14) Sandberg, I. W., "On the Response of Nonlinear Control Systems to Periodic Input Signals", The Bell System Technical Journal, Vol. XLIII, No. 3., May, 1964, pp. 911-926.

(15) Truxal, John G., Automatic Feedback Control System Synthesis. New York: McGraw-Hill Book Company, Inc., 1955. 675 pp.

(16) Zadeh, Lotfi A., and Charles A. Desoer, Linear System Theory. New York: McGraw-Hill Book Company, Inc., 1963. 628 pp.

APPENDIX A

Approximation to max $J_1(t)$

From equations (III-37) and (III-38) the expression, $\left[\Phi_*(u) - \Phi_{1*}(u)\right]$, becomes

$$\Phi_*(u) - \Phi_{1*}(u) = \frac{-e^{-(a-\lambda)u}}{1+e^{-(a-\lambda)T/2}} + \frac{4\sin(wu+\alpha_1)}{T\left[(a-\lambda)^2+w^2\right]^{\frac{1}{2}}} . \tag{A-1}$$

Consider an interval, $[u_1, u_2]$, in which $\left[\Phi_*(u) - \Phi_{1*}(u)\right]$ is positive and does not change sign. Then

$$\int_{u_1}^{u_2} \left|\Phi_*(u)-\Phi_{1*}(u)\right| du = \int_{u_1}^{u_2} \left[\Phi_*(u) - \Phi_{1*}(u)\right] du$$

$$= \int_{u_1}^{u_2} \left\{ \frac{-e^{-(a-\lambda)u}}{1+e^{-(a-\lambda)T/2}} + \frac{4\sin(wu+\alpha_1)}{T\left[(a-\lambda)^2+w^2\right]^{\frac{1}{2}}} \right\} du$$

$$= \frac{e^{-(a-\lambda)u_2} - e^{-(a-\lambda)u_1}}{(a-\lambda)\left[1+e^{-(a-\lambda)T/2}\right]} + \frac{2}{\pi\left\{(a-\lambda)^2+w^2\right\}^{\frac{1}{2}}} \times$$

$$\left[\cos(wu_1+\alpha_1) - \cos(wu_2+\alpha_1)\right] \quad ; \lambda \neq a .$$

$$= -\frac{1}{2}\left[u_2-u_1\right] + \frac{2}{\pi w}\left[\cos(wu_1)-\cos(wu_2)\right]; \lambda = a . \tag{A-2}$$

Similarily, in an interval, $[u_3, u_4]$, in which $\left[\Phi_*(u)-\Phi_{1*}(u)\right]$ is negative and does not change sign, then

$$\int_{u_3}^{u_4} \left|\Phi_*(u)-\Phi_{1*}(u)\right| du = \frac{e^{-(a-\lambda)u_3} - e^{-(a-\lambda)u_4}}{(a-\lambda)\left[1+e^{-(a-\lambda)T/2}\right]} - \frac{2/\pi}{\left\{(a-\lambda)^2+w^2\right\}^{\frac{1}{2}}} \times$$

$$\left[\cos(wu_4+\alpha_1) - \cos(wu_3+\alpha_1)\right] \quad ; \lambda \neq a .$$

$$= \frac{1}{2}\left[u_4 - u_3\right] + \frac{2}{\pi w}\left[\cos(wu_4) - \cos(wu_3)\right]; \quad \lambda = a \; . \tag{A-3}$$

The zeros of $\left[\Phi_*(u) - \Phi_{1*}(u)\right]$ can be found in the interval $[0, T/2]$ by using a rootfinding subroutine on a digital computer; and then equations (A-2) or (A-3) can be used (depending on the sign of $\left[\Phi_*(u) - \Phi_{1*}(u)\right]$) to determine the integral in the intervals between successive zeros. A summation of integrals will then yield $\int_0^{T/2} \left|\Phi_*(u) - \Phi_{1*}(u)\right| du$.

Also, equation (III-40) can be written as

$$\max_{0 \leq \tau \leq T/2} \left|f_*\left[x_{app}(\tau)\right]\right| = 1 + \lambda E, \quad \lambda > 0; \; E \geq 1$$

$$= 1 - |\lambda|, \quad \lambda < 0; \; 1 \leq E \leq \left\{1 + 2(1 - |\lambda|)/|\lambda|\right\}$$

$$= |\lambda| E - 1, \quad \lambda < 0; \; E \geq \left\{1 + 2(1 - |\lambda|)/|\lambda|\right\} . \tag{A-4}$$

Hence an approximation to $\max_{0 \leq t \leq T/2} |J_1(t)|$ is found.

Evaluation of $J_1(t)$

In order to evaluate $J_1(t)$, consideration must be given to the evaluation of the terms, $\phi_{1*}(t)$ and $\int_0^{T/2} \Phi_*(t-\tau) f_*\left[x_{app}(\tau)\right] d\tau$, of equation (III-44). When the input to the system, $\phi(t)$, is a sinusoid, then the operator equation (III-35) becomes

$$\phi_*(t) = \phi_{1*}(t) = \frac{p + a}{p + a - \lambda}\left[R \sin(wt - \theta)\right]$$

$$= \frac{R\left[w^2+a^2\right]^{\frac{1}{2}}}{\left[w^2+(a-\lambda)^2\right]^{\frac{1}{2}}} \sin(wt - \theta + \alpha_2), \tag{A-5}$$

where

$$\alpha_2 = \arctan\left[w/a\right] - \arctan\left[w/(a-\lambda)\right]. \tag{A-6}$$

It is noted that the time variable has been considered shifted so that the input sinusoid of the original system has a phase angle of $-\theta$ (θ is expressed in equation (III-8)), and the describing function approximation to the input to the nonlinearity is written

$$x_{app}(t) = E \sin wt, \tag{A-7}$$

now with zero phase angle.

The kernel of the transformed system, $\Phi_*(t-\tau)$, is expressed as

$$\Phi_*(t-\tau) = \frac{-e^{-(a-\lambda)(t-\tau)}}{1+e^{-(a-\lambda)T/2}} \quad ; \quad 0 \leq t-\tau \leq T/2$$

$$= \frac{e^{-(a-\lambda)T/2}\, e^{-(a-\lambda)(t-\tau)}}{1+e^{-(a-\lambda)T/2}} \quad ; \quad 0 \leq \tau - t \leq T/2 \tag{A-8}$$

so that the integral in equation (III-44) can be written as

$$\int_0^{T/2} \Phi_*(t-\tau) f_*\left[x_{app}(\tau)\right] d\tau = \int_0^{t} \frac{-e^{-(a-\lambda)(t-\tau)}}{1+e^{-(a-\lambda)T/2}} f_*\left[x_{app}(\tau)\right] d\tau$$

$$+ \int_t^{T/2} \frac{e^{-(a-\lambda)T/2}\, e^{-(a-\lambda)(t-\tau)}}{1+e^{-(a-\lambda)T/2}} f_*\left[x_{app}(\tau)\right] d\tau . \tag{A-9}$$

Now the transformed nonlinearity is simply

$$f_*\left[x_{app}(\tau)\right] = f_*\left[E \sin(w\tau)\right] = (1+\lambda)E \sin w\tau \; ; \; 0 \leq \tau \leq \frac{\arcsin(1/E)}{w}$$

$$= 1 + \lambda E \sin w\tau \; ; \; \frac{\arcsin(1/E)}{w} \leq \tau \leq \frac{\pi - \arcsin(1/E)}{w}$$

$$= (1+\lambda)\, E \sin w\tau; \; \frac{\pi - \arcsin(1/E)}{w} \leq \tau \leq T/2 \; .$$

(A-10)

The integral represented by equation (A-9) can then be evaluated for each of the three cases $0 \leq t \leq \frac{\arcsin(1/E)}{w}$, $\frac{\arcsin(1/E)}{w} \leq t \leq \frac{\pi - \arcsin(1/E)}{w}$, and $\frac{\pi - \arcsin(1/E)}{w} \leq t \leq T/2$.

The result is

$$\int_0^{T/2} \Phi_*(t-\tau) f_*\left[x_{app}(\tau)\right] d\tau = \frac{Ee^{-a_*t}\left\{-w\cos(w\tau_1)\left[e^{-a_*\tau_1} + e^{-a_*\tau_2}\right] + \frac{w^2}{a_*E}\left[e^{-a_*\tau_1} - e^{-a_*\tau_2}\right]\right\}}{(a_*^2+w^2)(1+e^{-a_*T/2})}$$

$$\frac{-(1+\lambda)a_*E}{a_*^2+w^2} \sin wt + \frac{(1+\lambda)wE}{a_*^2+w^2} \cos wt \; ; \quad 0 \leq t \leq \tau_1$$

$$= \frac{Ee^{-a_*t}\left\{w\cos(w\tau_1)\left[e^{a_*\tau_1} - e^{-a_*\tau_1}\right] + \frac{w^2}{a_*E}\left[e^{a_*\tau_1} + e^{-a_*\tau_1}\right]\right\}}{(a_*^2+w^2)(1+e^{-a_*T/2})}$$

$$\frac{-1}{a_*} - \frac{\lambda E a_*}{a_*^2+w^2} \sin wt + \frac{\lambda E w}{a_*^2+w^2} \cos wt \; ; \; \tau_1 \leq t \leq \tau_2$$

$$= \frac{Ee^{-a_*t}\left\{w\cos(w\tau_1)\left[e^{a_*\tau_1} + e^{a_*\tau_2}\right] + \frac{w^2}{Ea_*}\left[e^{a_*\tau_1} - e^{a_*\tau_2}\right]\right\}}{(a_*^2+w^2)(1+e^{-a_*T/2})}$$

$$\frac{-(1+\lambda)a_*E}{a_*^2+w^2} \sin wt + \frac{(1+\lambda)Ew}{a_*^2+w^2} \cos wt; \; \tau_2 \leq t \leq T/2$$

(A-11)

where

$$\tau_1 = \frac{\arcsin(1/E)}{w} \; ; \quad \tau_2 = \frac{-\arcsin(1/E)}{w} \; ; \quad a_* = a - \lambda \; . \tag{A-12}$$

Application of equations (A-5), (A-7), and (A-11) to equation (III-44) then yields an expression for $J_1(t)$ in the interval $0 \leq t \leq T/2$.

Minimization of M_*I_*

The expressions for M_*I_* are given in equation (III-33). Since

$$\lim_{\lambda \to -\infty} \left\{ \tanh \left[\frac{(a + |\lambda|)\pi}{2w} \right] \right\} = 1 \tag{A-13}$$

and

$$\lim_{\lambda \to -\infty} \left\{ \frac{|\lambda|}{a + |\lambda|} \right\} = 1 \; , \tag{A-14}$$

it is easily seen that in the range $-\infty \leq \lambda \leq -\frac{1}{2}$, M_*I_* is minimum for $\lambda = -\frac{1}{2}$. Thus it is sufficient to find $\min_{-\frac{1}{2} \leq \lambda \leq \infty} \{M_*I_*\}$.

Extremal points for M_*I_* in the interval $-\frac{1}{2} \leq \lambda \leq \infty$ must satisfy

$$\tanh^2\left[\frac{(a - \lambda)\pi}{2w}\right] + \left\{ \frac{(1 + a)2w}{(1 + \lambda)(a - \lambda)\pi} \right\} \tanh\left[\frac{(a-\lambda)\pi}{2w}\right] - 1 = 0 \; . \tag{A-15}$$

Also,

$$\lim_{\lambda \to \infty} \left\{ \frac{1 + \lambda}{a - \lambda} \tanh\left[\frac{(a - \lambda)\pi}{2w}\right] \right\} = 1 \; . \tag{A-16}$$

It is obvious that the value of $\min_{-\frac{1}{2} \leq \lambda \leq \infty} \{ M_*I_* \}$ will always be less than 1 so that the λ corresponding to the absolute minimum will always be finite. A digital computer

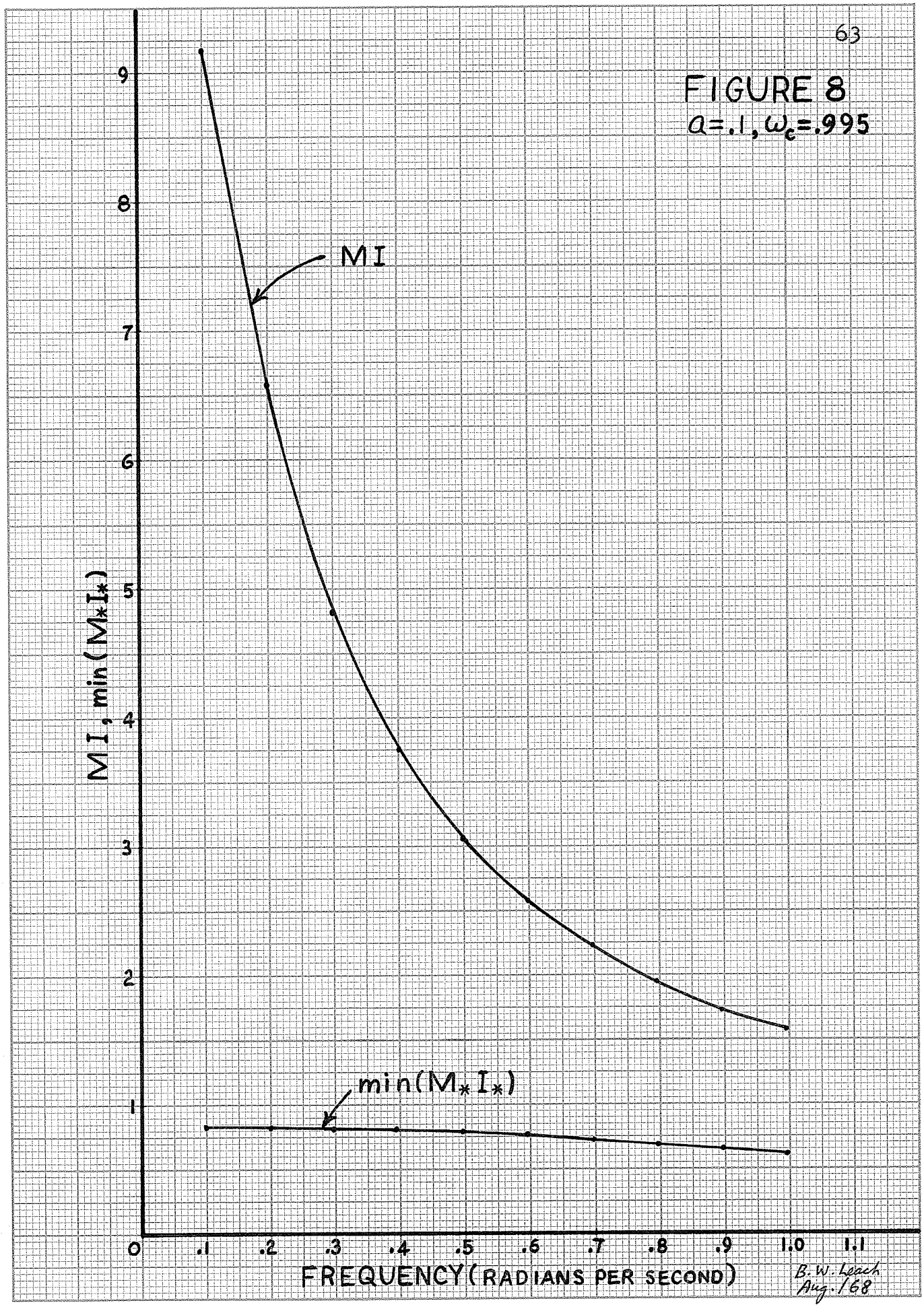

can be used to solve equation (A-15) for all extremal points, and each one can be tested to find the λ corresponding to min $\{M_*I_*\}$.

Results of M_*I_* investigation

A number of typical first order systems in the range $0 \leq a \leq .1$ were investigated to find min $\{M_*I_*\}$. One interesting result of the investigation was the fact that for every system studied the value of λ corresponding to min $\{M_*I_*\}$ was found to be -.5. This occurred for all frequencies in the range of interest, $\frac{w_c}{10} \leq w \leq w_c$.

It thus appears that a minimization of M_* is sufficient to minimize M_*I_*, at least in the region of interest. Obviously then, the change of I_* with λ is quite slow compared to the linear change with λ of M_*. Figure 8 shows a plot of MI and min$\{M_*I_*\}$ versus frequency in the region $\frac{w_c}{10} \leq w \leq w_c$ to indicate the typical decrease in value that results when the linear rotation is applied.

Investigation of error estimate minimization

It was suspected that the value of λ yielding min $\{M_*I_*\}$ might also yield the minimum bounds. This idea was pursued by investigating several first order systems and actually calculating the bound (for both approximate max $|J_1(t)|$ and exact max $|J_1(t)|$) as λ was iterated slowly through the range in which the minimum bound was known to lie. In all

cases, for frequencies in the range $\frac{w_c}{10} \leq w \leq w_c$, the minimum bound occurred for $\lambda = -.5$, as suspected. It was noted, however, that for frequencies larger than w_c, where a bound would exist even without the use of the linear rotation, it was not necessarily true that the λ to minimize the bound was always -.5. It thus appears that in the region of interest, $\frac{w_c}{10} \leq w \leq w_c$, M_*I_* is the critical term in determining the bound and must change much more drastically with λ than does $\max|J_1(t)|$.

The foregoing observations indicate that the process of determining the minimum bound for the first order case in the region of interest is not as difficult as first was thought. Fortunately, λ_{opt} is always the same and the calculation of the minimum bound becomes relatively straightforward.

APPENDIX B

Minimization of M_*I_*

M_*I_* was minimized for a variety of second order systems in the particular range $0 \leq a \leq 1$; $.5 \leq K \leq 10$. The most important result was the fact that the minimization did not always produce $\min_{\lambda} \{M_*I_*\} < 1$. As a matter of fact, it was only for a few systems investigated that $\min_{\lambda} \{M_*I_*\} < 1$ in the complete range $\frac{w_c}{10} \leq w \leq w_c$. It should be noted that $\lim_{|\lambda| \to \infty} \{M_*I_*\} = 1$, so that $\min_{\lambda} \{M_*I_*\}$ is always 1 or less. However, in a case where $\min_{\lambda} \{M_*I_*\} = 1$, the Garber-Rozenvasser bound obviously cannot be applied, since it will approach infinity.

It was also noticed that in cases where $\min_{\lambda} \{M_*I_*\} < 1$ the value of λ producing the minimum was always $-.5$. Since a similar result had been found for first order systems, this tended to confirm the idea that a minimization of M_* would also minimize M_*I_* under certain conditions.

Figures 9 and 10 show plots of MI and $\min\{M_*I_*\}$ versus frequency to indicate the large decrease caused by the application of linear rotation. Figure 9 is an example of the case where $\min \{M_*I_*\} < 1$ for the complete range $\frac{w_c}{10} \leq w \leq w_c$, so that an error bound can be found in this entire range. On the other hand, Figure 10 is an example of the case where $\min \{M_*I_*\} < 1$ only over part of the range. Thus a bound cannot be found over the whole range of interest in this instance.

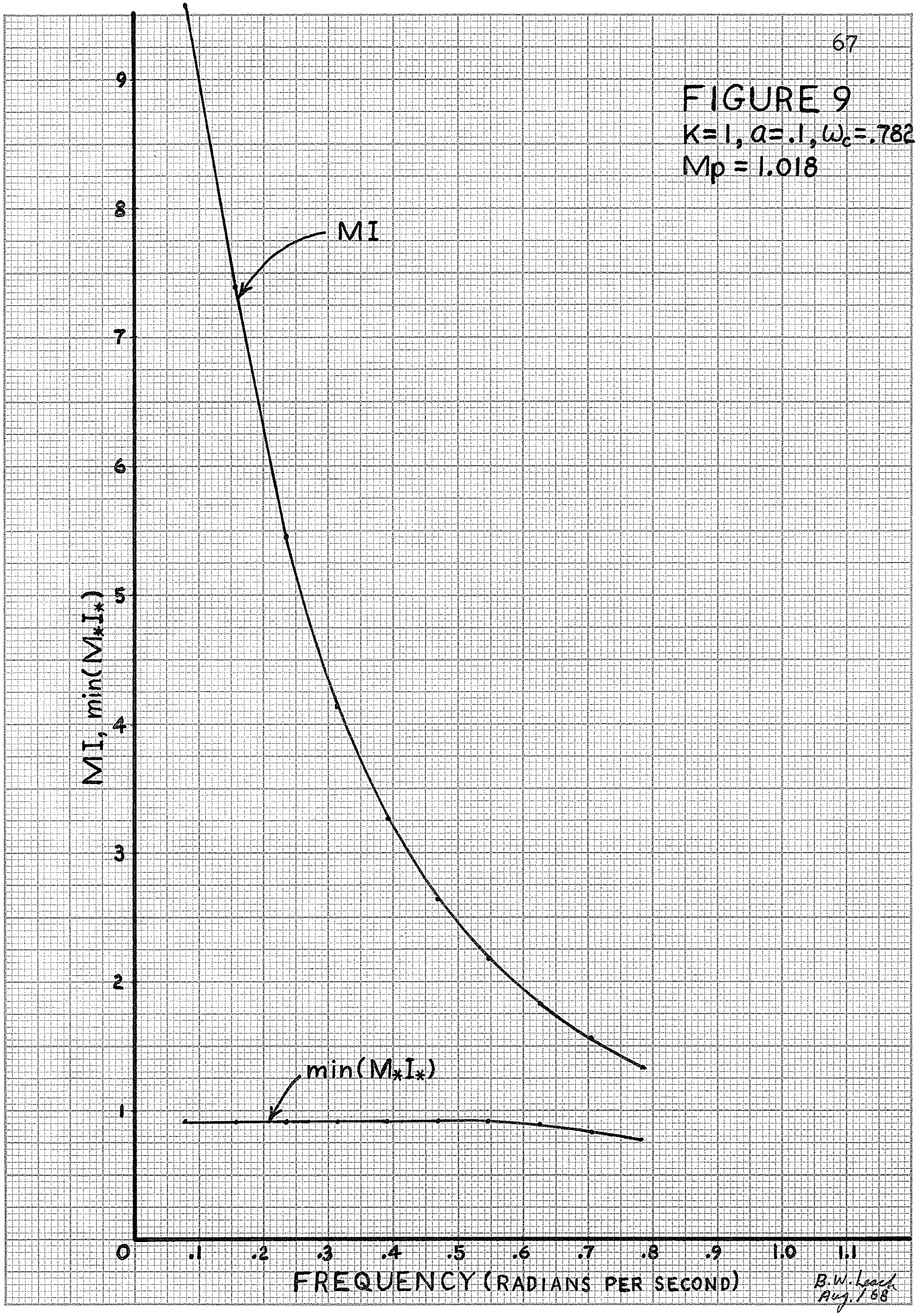

FIGURE 9
K=1, a=.1, ω_c=.782
Mp = 1.018

B.W. Leach
Aug. '68

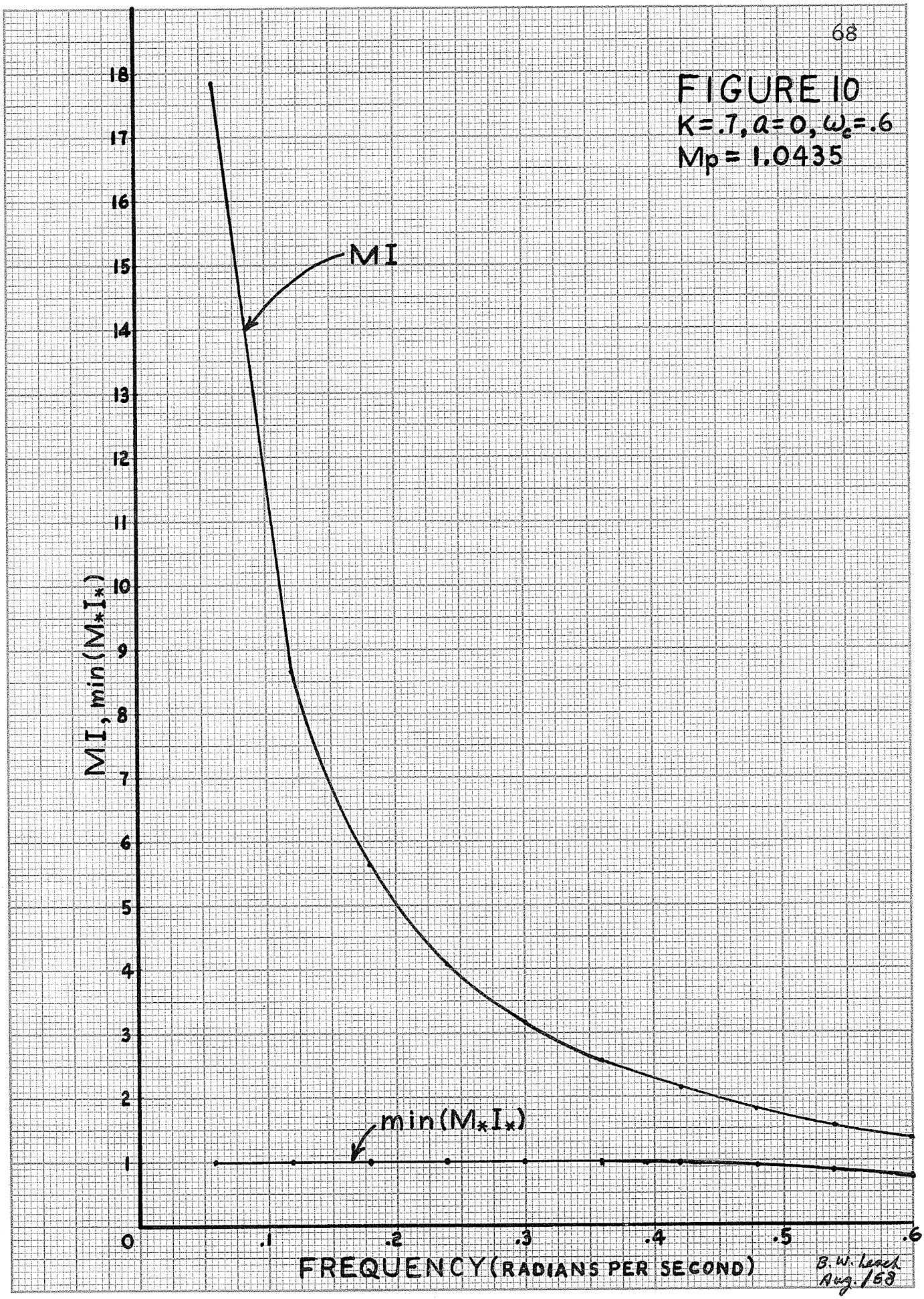

The case where the Garber-Rozenvasser bound could not be applied over any of the frequency region of interest was found to occur most often in the investigation of $\min\{M_* I_*\}$ for typical systems. The case normally occurred as the parameter k was being increased while a remained constant, or while a was being decreased while k remained constant.

Minimization of error estimate

For those cases in which the bound could be applied, an investigation was made to discover whether or not the minimization of $M_* I_*$ would also minimize the bound. This was found to be correct, and since $\lambda = -.5$ was always the optimum value, meant that the calculation of the bound was reasonably straightforward.